An aerial photograph showing a large landslide that has partially covered a two-lane road. The landslide material is dark and appears to be a mix of soil and rock. Several vehicles, including a yellow school bus and a white car, are visible on the road. The surrounding area is a mix of green trees and brown, dry vegetation.

Assessment of Landslide Impacts Along Oregon Lifelines

Ben Leshchinsky, Michael Olsen and Nick Mathews
Oregon State University



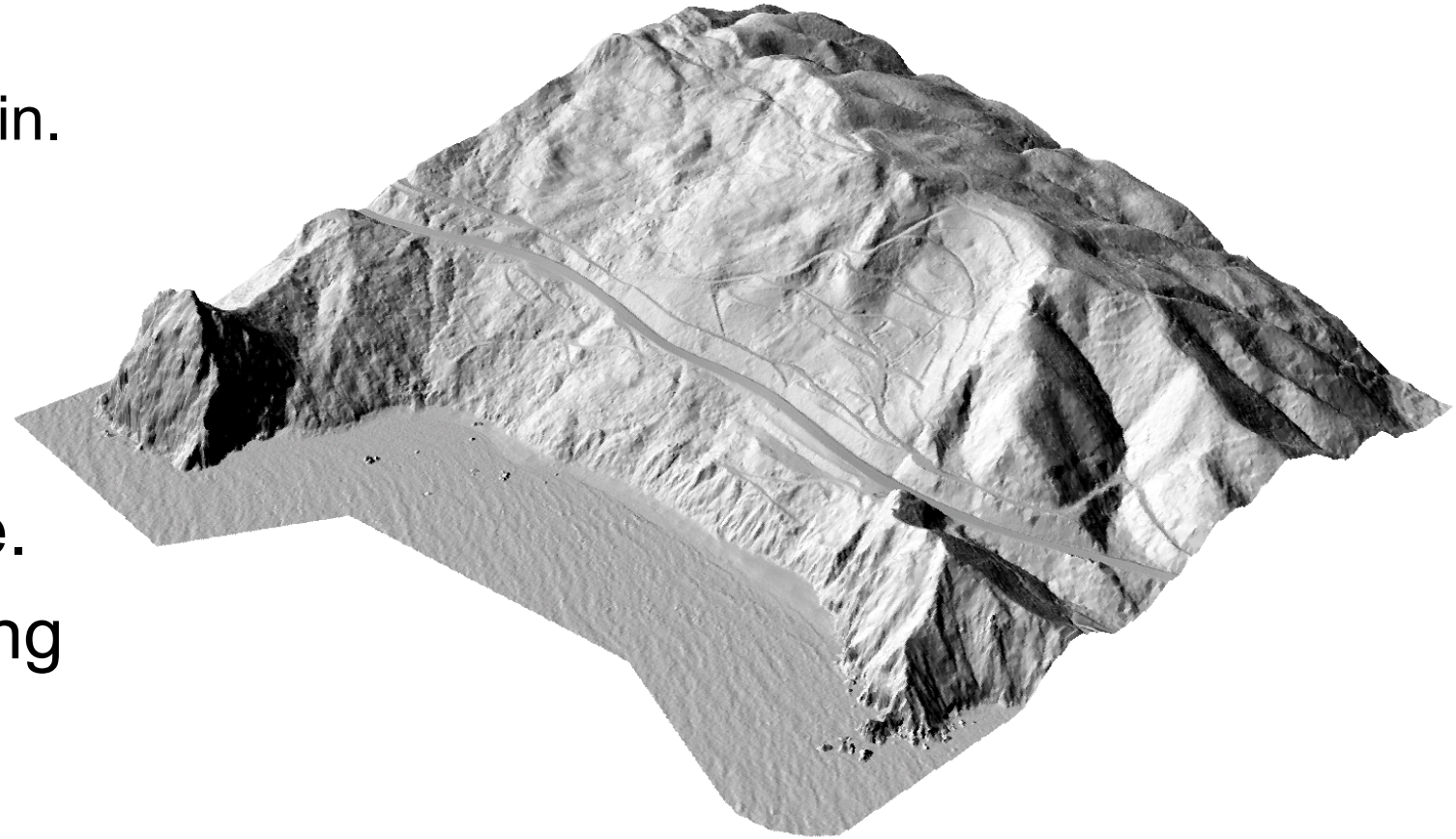
Landslides in Oregon

- Landslides are a major source of infrastructure damage in the Pacific Northwest.
- Landslides are a negative geotechnical asset; their mitigation is also an asset. Both are too often forgotten...
- Avoiding or absorbing damage in geotechnical assets achieved through:
 - Expanded attention to monitoring
 - Cataloguing landslides and assets for analysis
 - Using advanced in-situ and remotely-sensed data to interpret landforms
 - Using data-driven models to understand landslide impacts
- Overview of a climate- and seismic-focused project focused on landslide impacts.



Lidar as an asset.

- Detailed topography for:
 - Stability analyses.
 - Identification of unstable terrain.
 - High-resolution change.
- Can be integrated with geospatial information about infrastructure, development, homes, population and more.
- Particularly useful for mapping past landslide features.
- ***Great!!! ... Now what?***

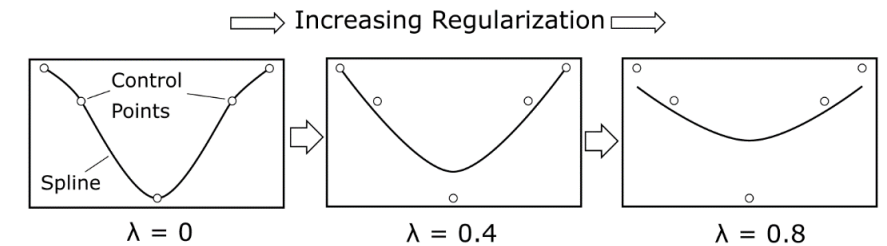
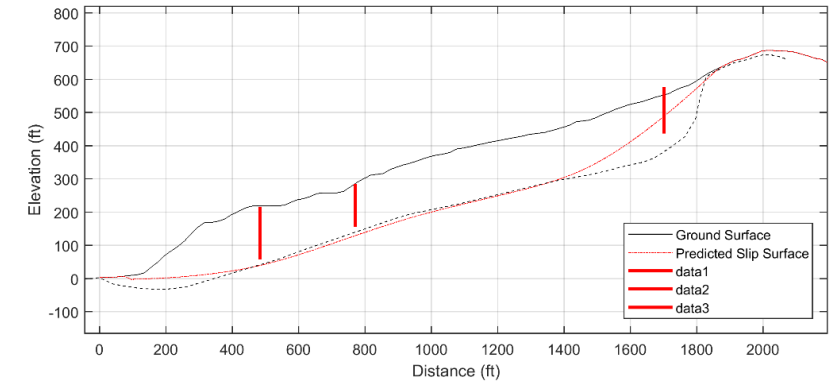
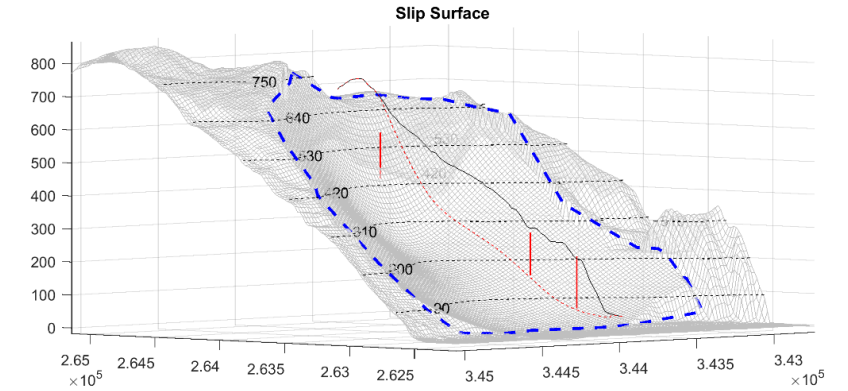


Back-Analyses of Landslides

- Lidar DTMs very applicable to interpreting singular events.
- Through sensitivity analyses and use of landslide inventories, we can explore regional trends in landslide characteristics.
- Herein, we introduce an approach to:
 - Infer landslide slip surface geometry for entire landslide inventories
 - Reconstruct pre-failure topography for landslides
 - Perform 3D back-analyses on thousands of landslides
 - Infer spatial trends of strength associated with specific geologies, regions, materials, etc.

Hybrid Thin-Plate Spline

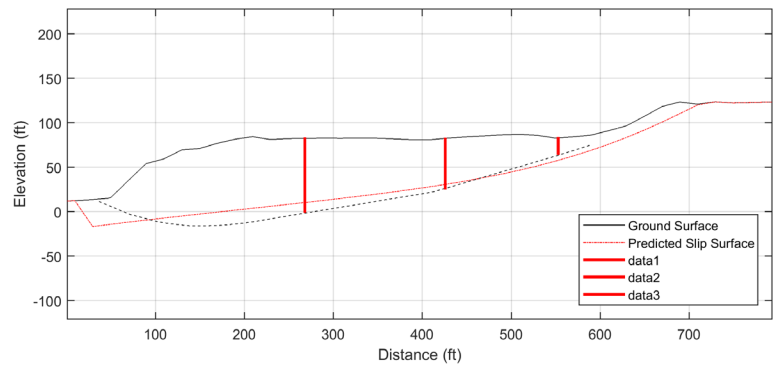
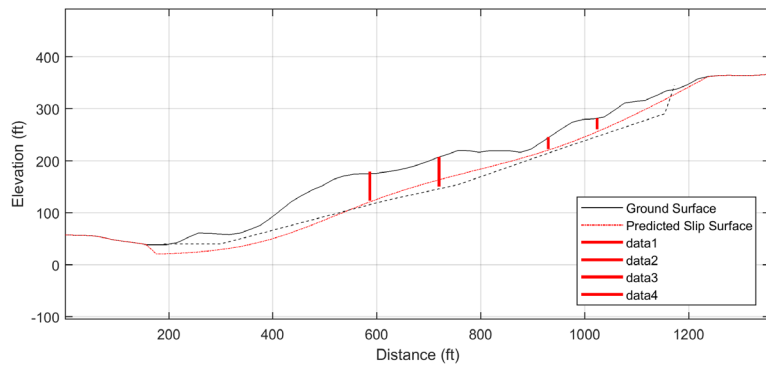
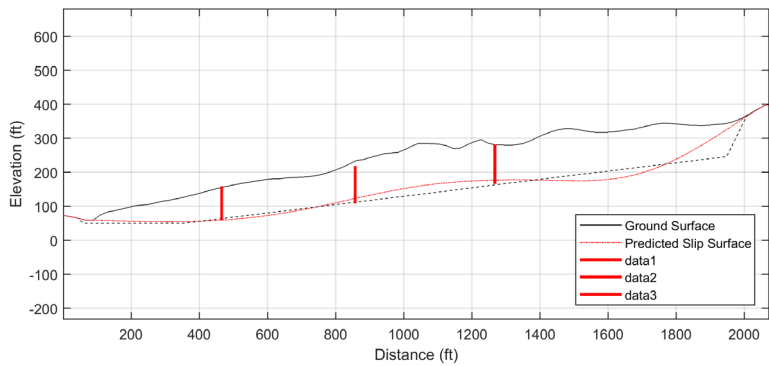
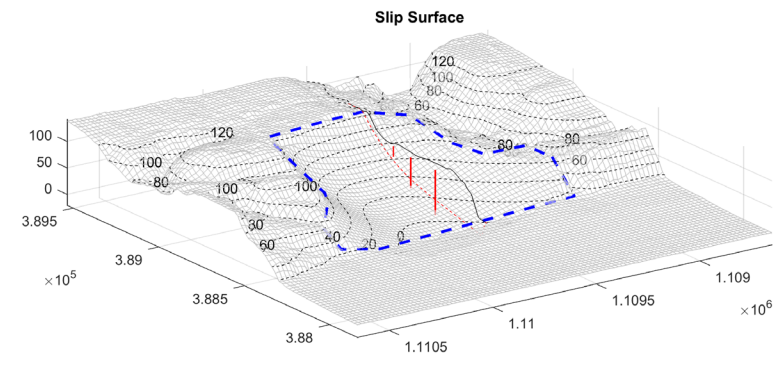
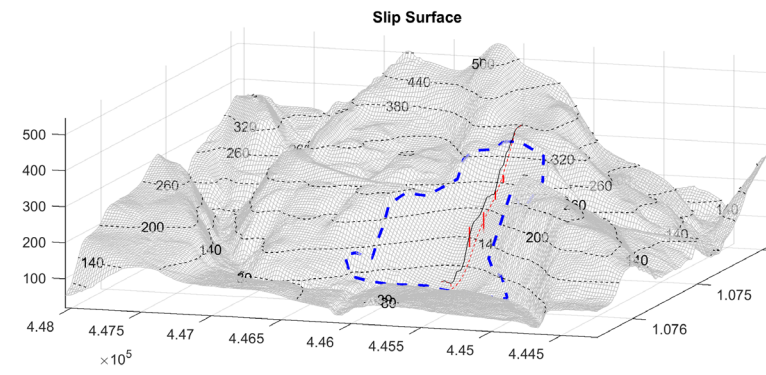
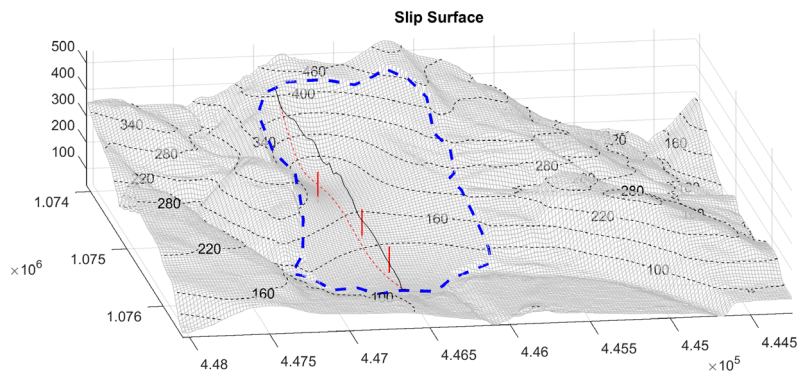
- We leverage high-resolution lidar topographic data to analyze these large datasets.
- We use a modified thin-plate spline (TPS) to use main scarps, landslide deposits to infer rupture surface geometry (Bunn et al. 2020).
- TPS capable of producing complex shapes found in landslide slip surfaces.
- TPS may reduce complexity through regularization of boundary conditions.



Bunn, M., Leshchinsky, B., & Olsen, M. J. (2020). Estimates of three-dimensional rupture surface geometry of deep-seated landslides using landslide inventories and high-resolution topographic data. *Geomorphology*, 367, 107332.

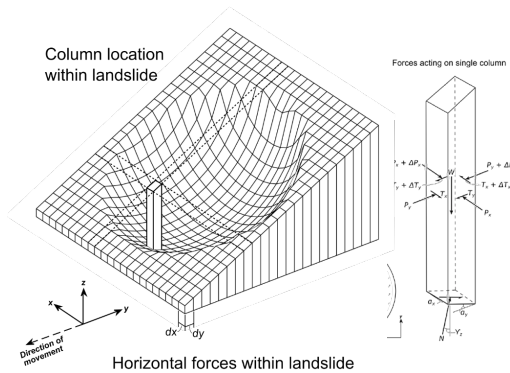
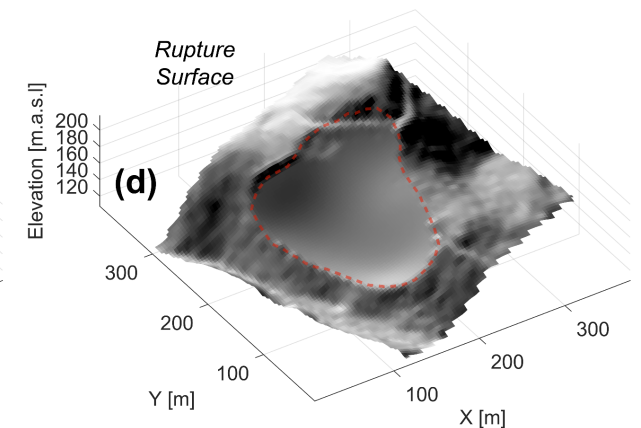
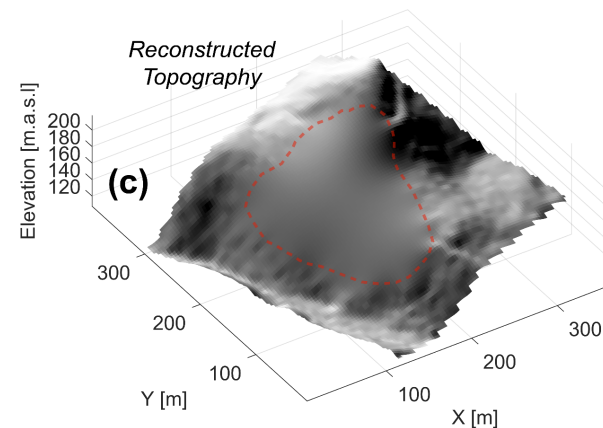
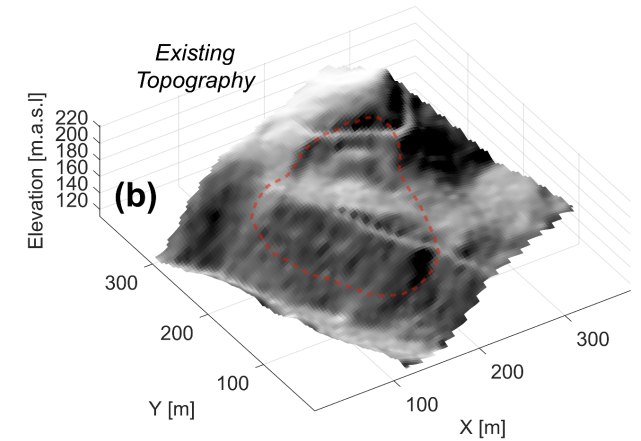
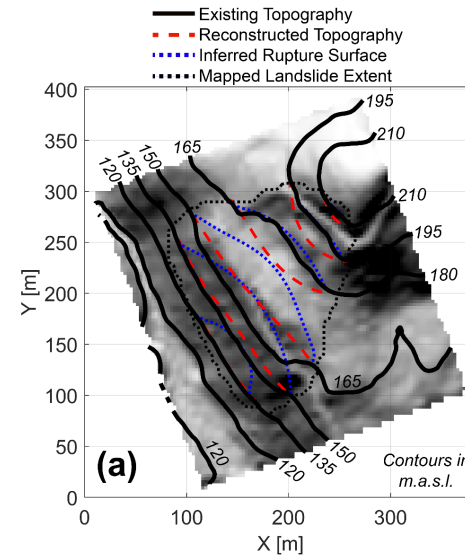
Alberti, S., Leshchinsky, B., Roering, J., Perkins, J., & Olsen, M. J. (2022). Inversions of landslide strength as a proxy for subsurface weathering. *Nature Communications*, 13(1), 6049.

- Applied to series of well-characterized landslides to calibrate regularization, resolution, projection constraints.



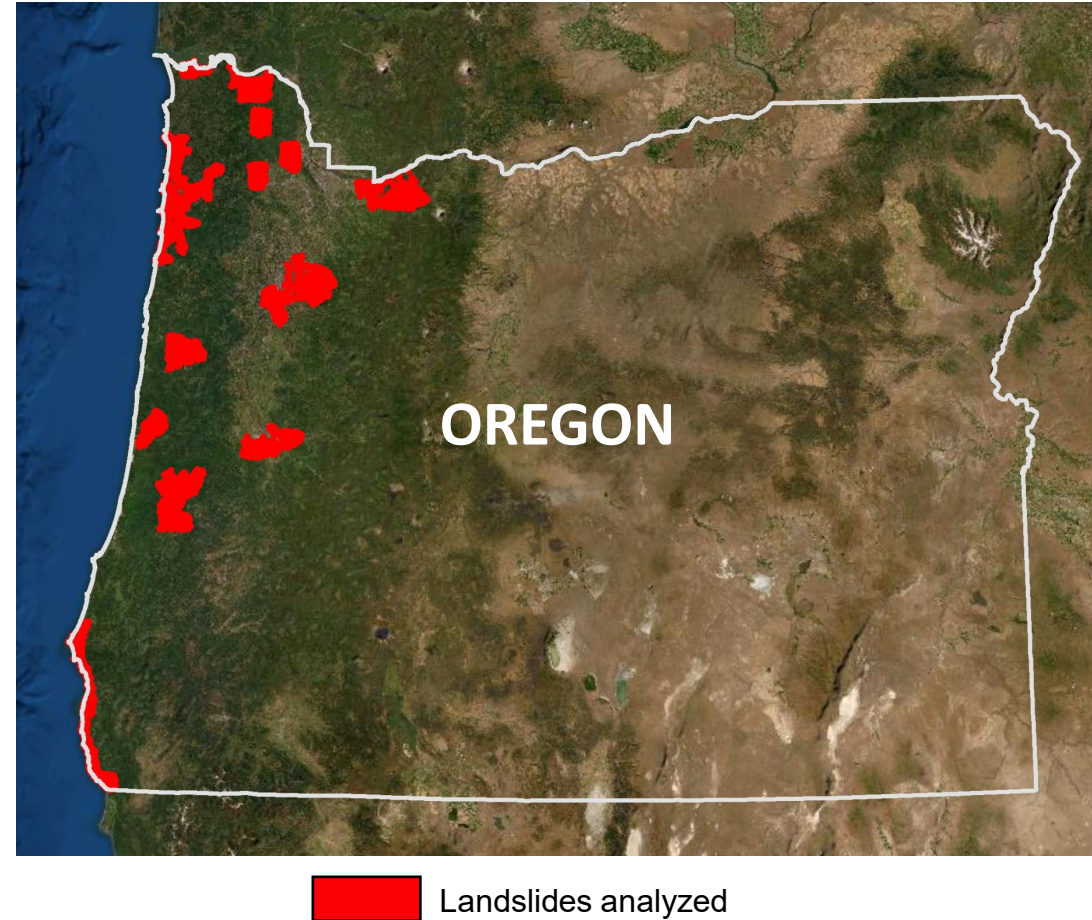
Reconstruction of Surface Geometry

- Similar procedures may also be applied to reconstruct pre-failure surface geometry.
- Done through ignoring landslide extents and infilling from surrounding “unfailed” terrain.



Application to Landslide Inventories

- We gathered high-quality landslide inventories in Oregon (DOGAMI SLIDO).
- Reconstruct failure geometries from each inventory to glean trends in geologic unit, geometry, mechanism, strength.
- Performed on landslides w/ limited estimated evacuation.
- Overall, we used >7,300 landslides in our analysis.

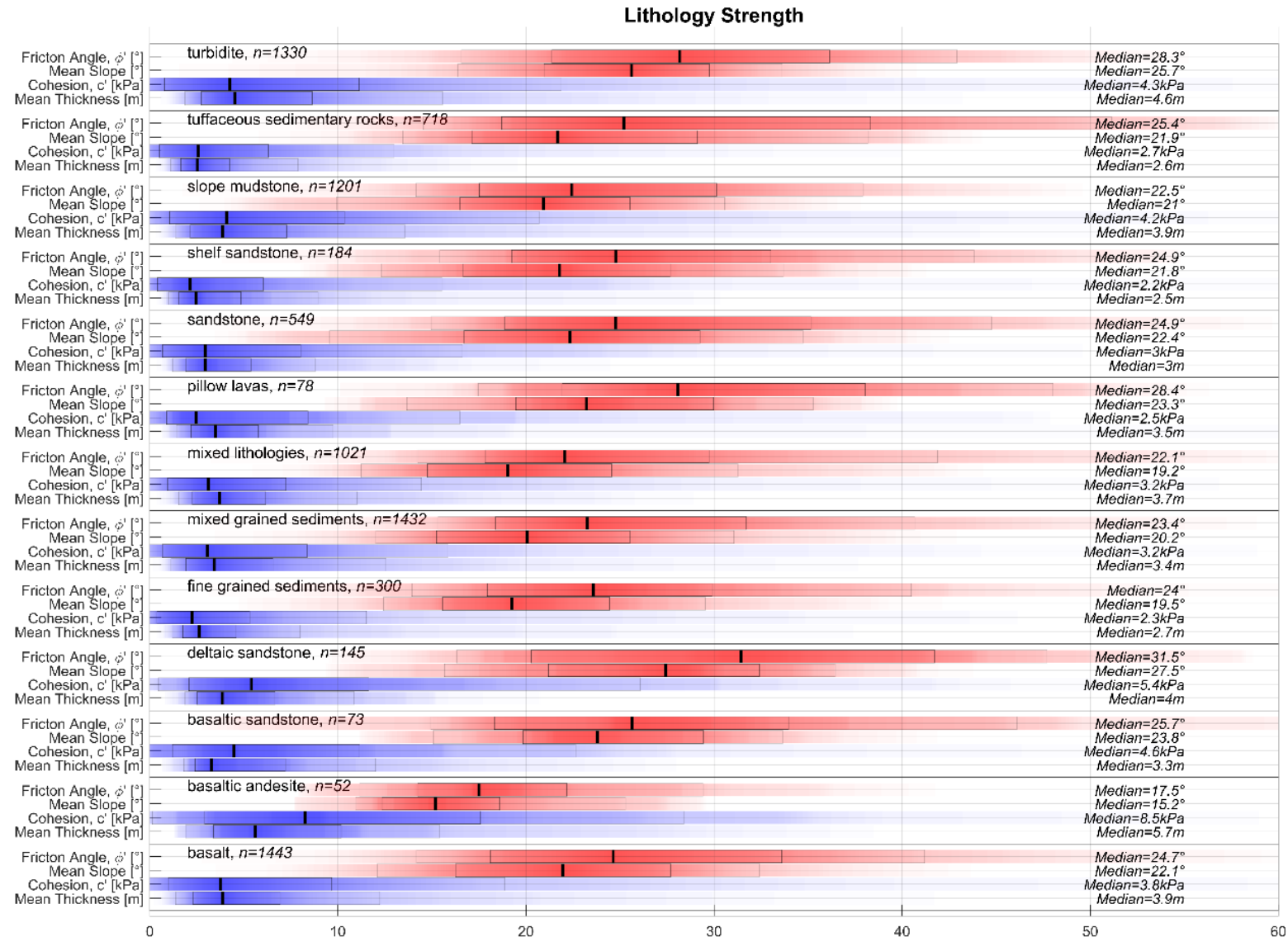


Bunn, M., Leshchinsky, B., & Olsen, M. J. (2020). Geologic Trends in Shear Strength Properties Inferred Through Three-Dimensional Back Analysis of Landslide Inventories. *Journal of Geophysical Research: Earth Surface*, 125(9), e2019JF005461.

Bunn, M., Leshchinsky, B., & Olsen, M. J. (2020). Estimates of three-dimensional rupture surface geometry of deep-seated landslides using landslide inventories and high-resolution topographic data. *Geomorphology*, 367, 107332.

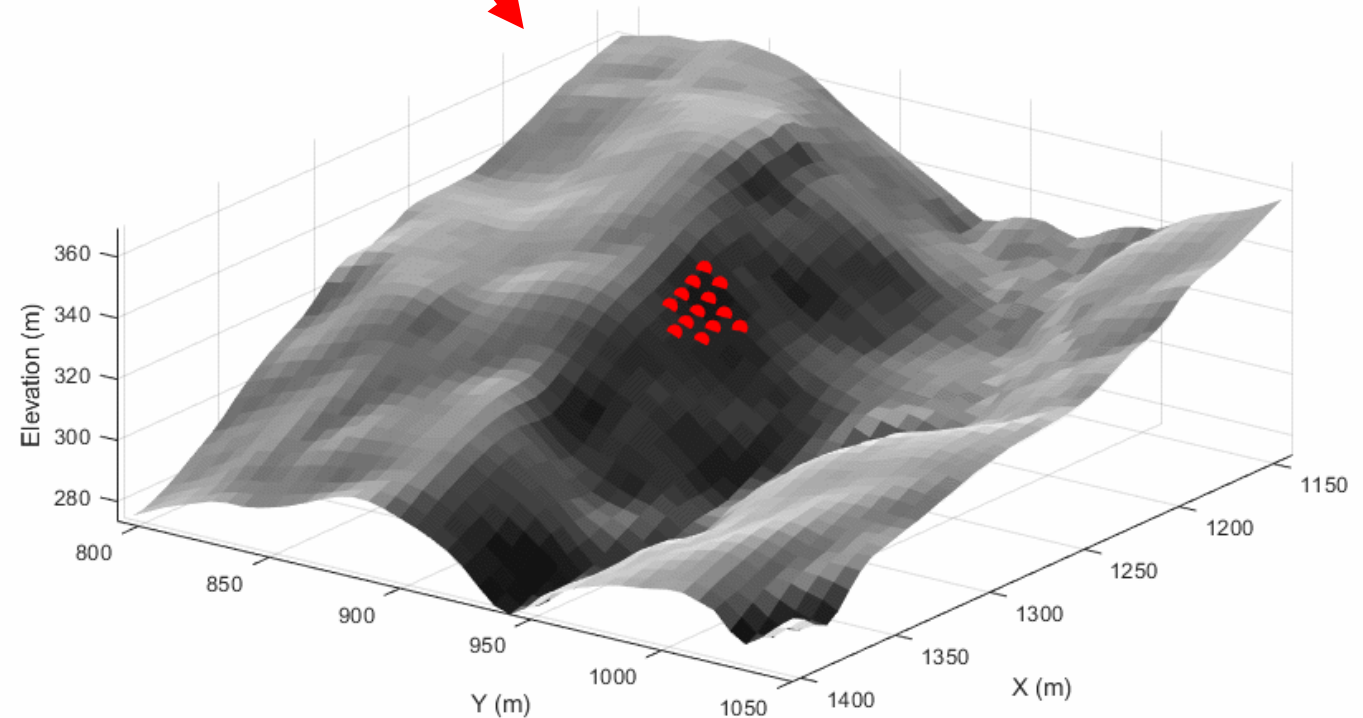
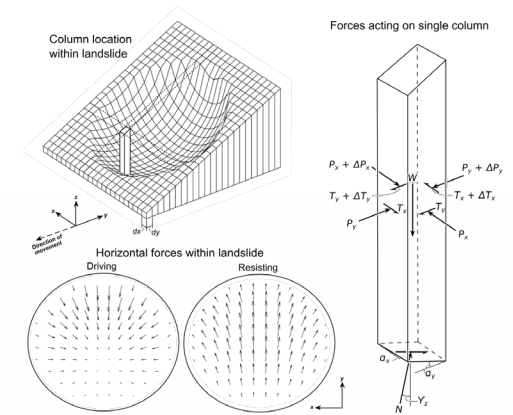
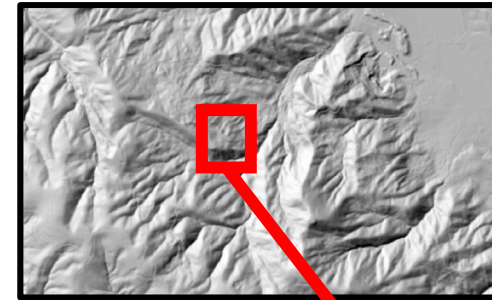
Lithology

- Can take geologic classifications and have associated strength properties!
- Can take typical lithologic units and begin to characterize differences in strength, morphology, etc.
- Can be used in forward-facing models!



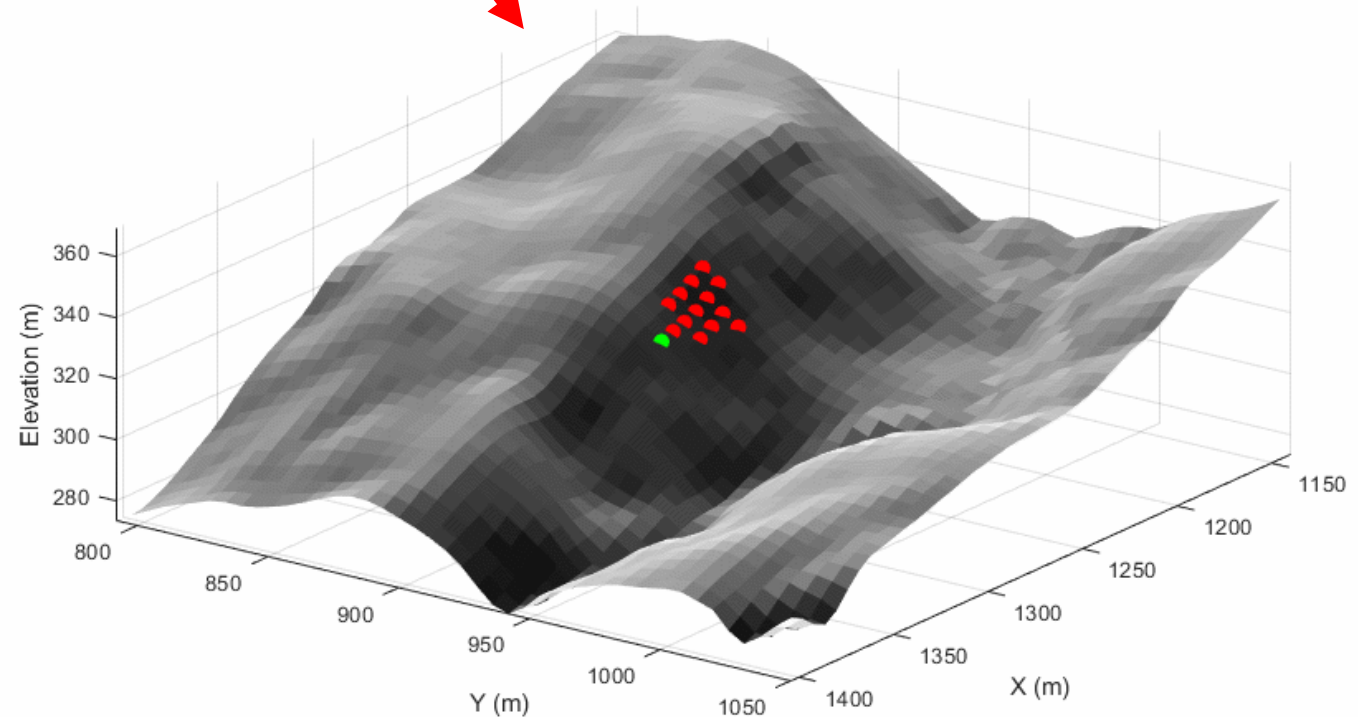
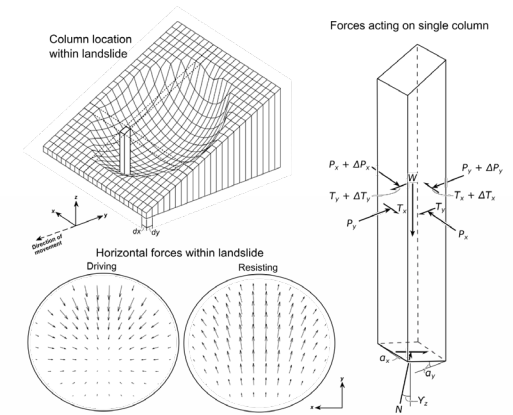
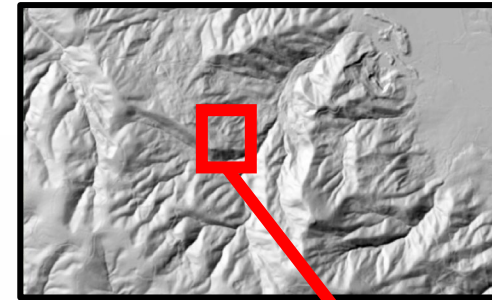
Susceptibility

- 1) Characterizes discrete landslide volumes – triggered by rainfall or earthquakes
- 2) Identify unstable clusters using 3D limit equilibrium
- 3) Achieve force equilibrium by accumulating downslope cells of soil



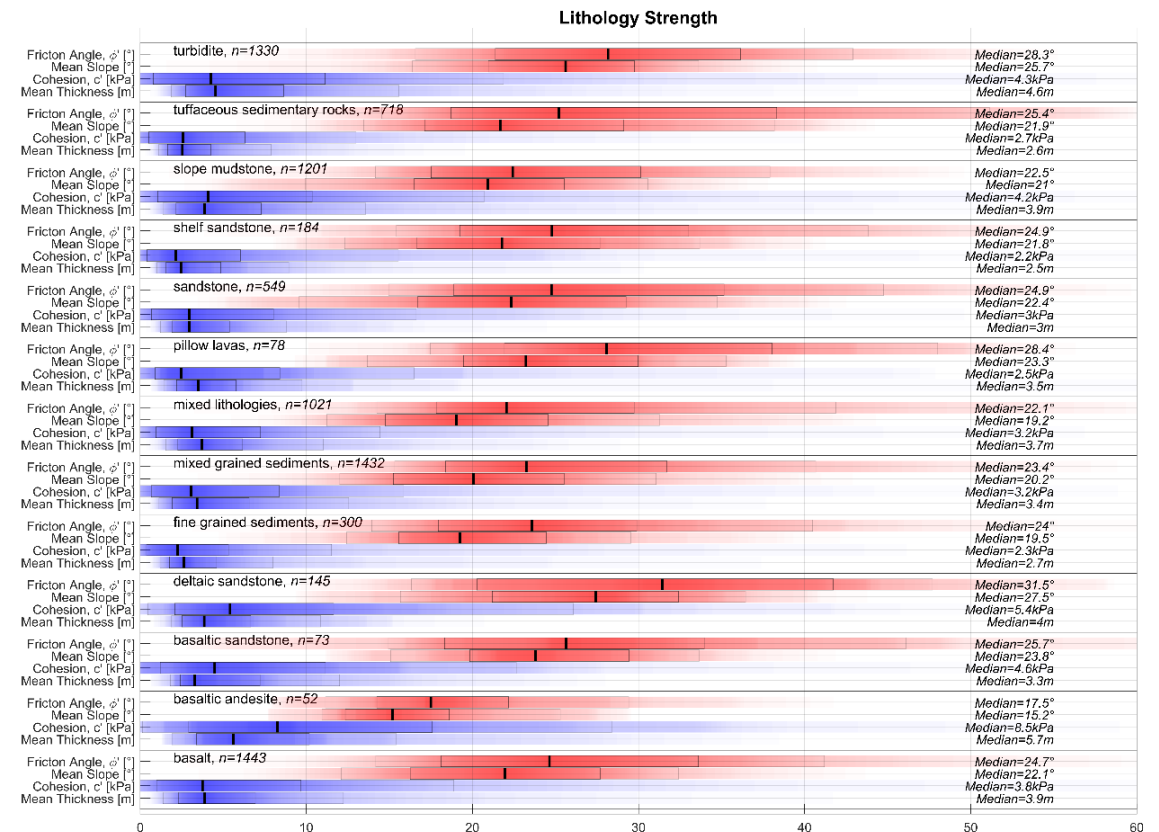
Susceptibility

- 1) Characterizes discrete landslide volumes – triggered by rainfall or earthquakes
- 2) Identify unstable clusters using 3D limit equilibrium
- 3) Achieve force equilibrium by accumulating downslope cells of soil



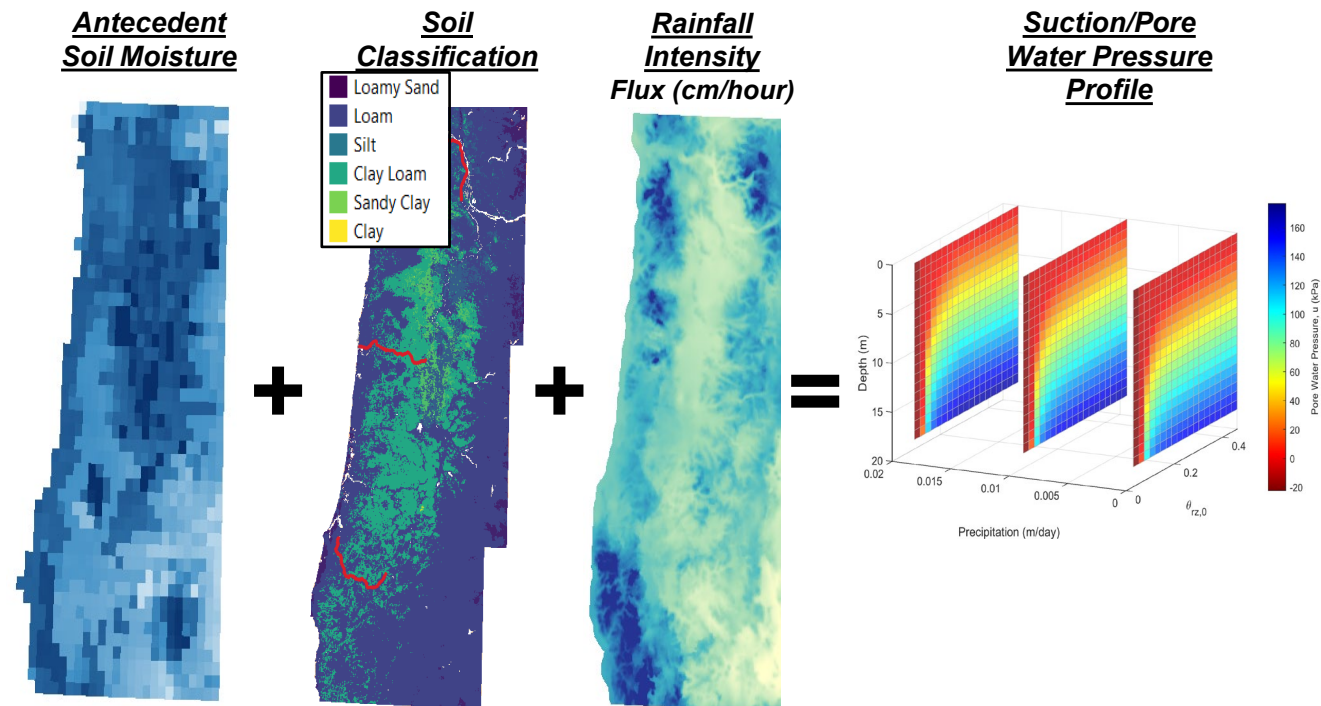
Inputs

- Strength
 - Distribution determined from forensics code.
- Soil Moisture, Unsaturated Properties
 - Soil moisture time series from NASA SMAP satellite data (daily)
 - SoilGrids, Rosetta GeoTransfer Function
- Estimated Soil Depth
 - Roering (2006) hillslope evolution model
- High-resolution DTM
 - OLC 3 ft. lidar, 1068 km²
- Intensity-duration precipitation for storm recurrence interval
 - ODOT hydraulics manual (e.g. 10 year storm)
- Seismic Event PGA map
 - OHELP, (Sharifi et al. 2016)



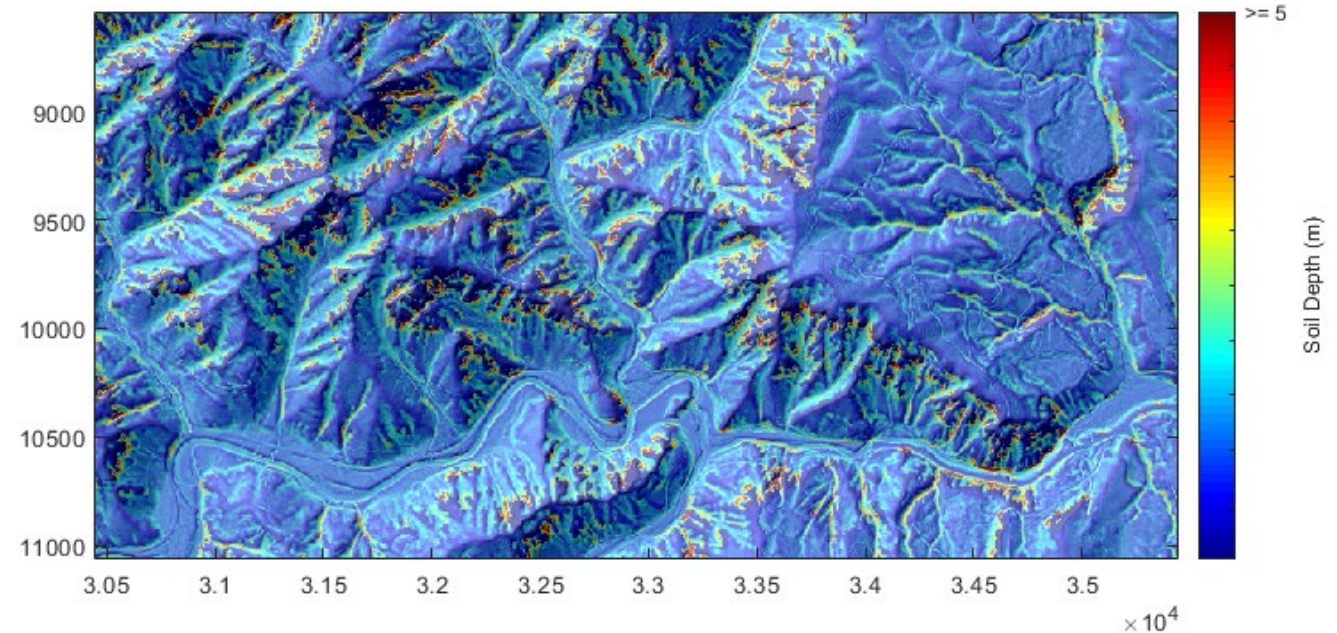
Inputs

- Strength
 - Distribution determined from forensics code.
- Soil Moisture, Unsaturated Properties
 - Soil moisture time series from NASA SMAP satellite data (daily)
 - SoilGrids, Rosetta GeoTransfer Function
- Estimated Soil Depth
 - Roering (2006) hillslope evolution model
- High-resolution DTM
 - OLC 3 ft. lidar, 1068 km²
- Intensity-duration precipitation for storm recurrence interval
 - ODOT hydraulics manual (e.g. 10 year storm)
- Seismic Event PGA map
 - OHELP, (Sharifi et al. 2016)



Inputs

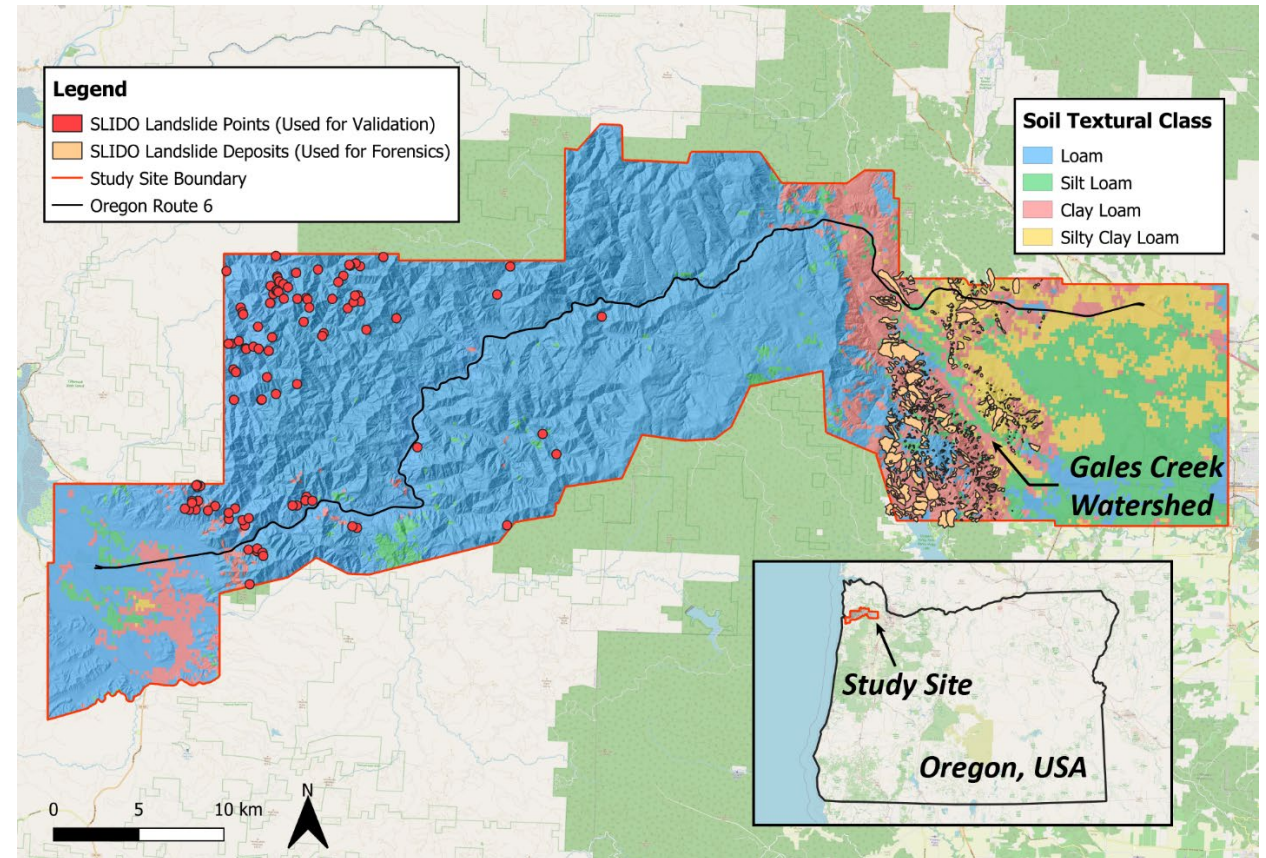
- Strength
 - Distribution determined from forensics code.
- Soil Moisture, Unsaturated Properties
 - Soil moisture time series from NASA SMAP satellite data (daily)
 - SoilGrids, Rosetta GeoTransfer Function
- Estimated Soil Depth
 - Roering (2006) hillslope evolution model
- High-resolution DTM
 - OLC 3 ft. lidar, 1068 km²
- Intensity-duration precipitation for storm recurrence interval
 - ODOT hydraulics manual (e.g. 10 year storm)
- Seismic Event PGA map
 - OHELP, (Sharifi et al. 2016)



Thinner soil mantle in high curvature areas helps constrain landslides to faces and typical areas of instability

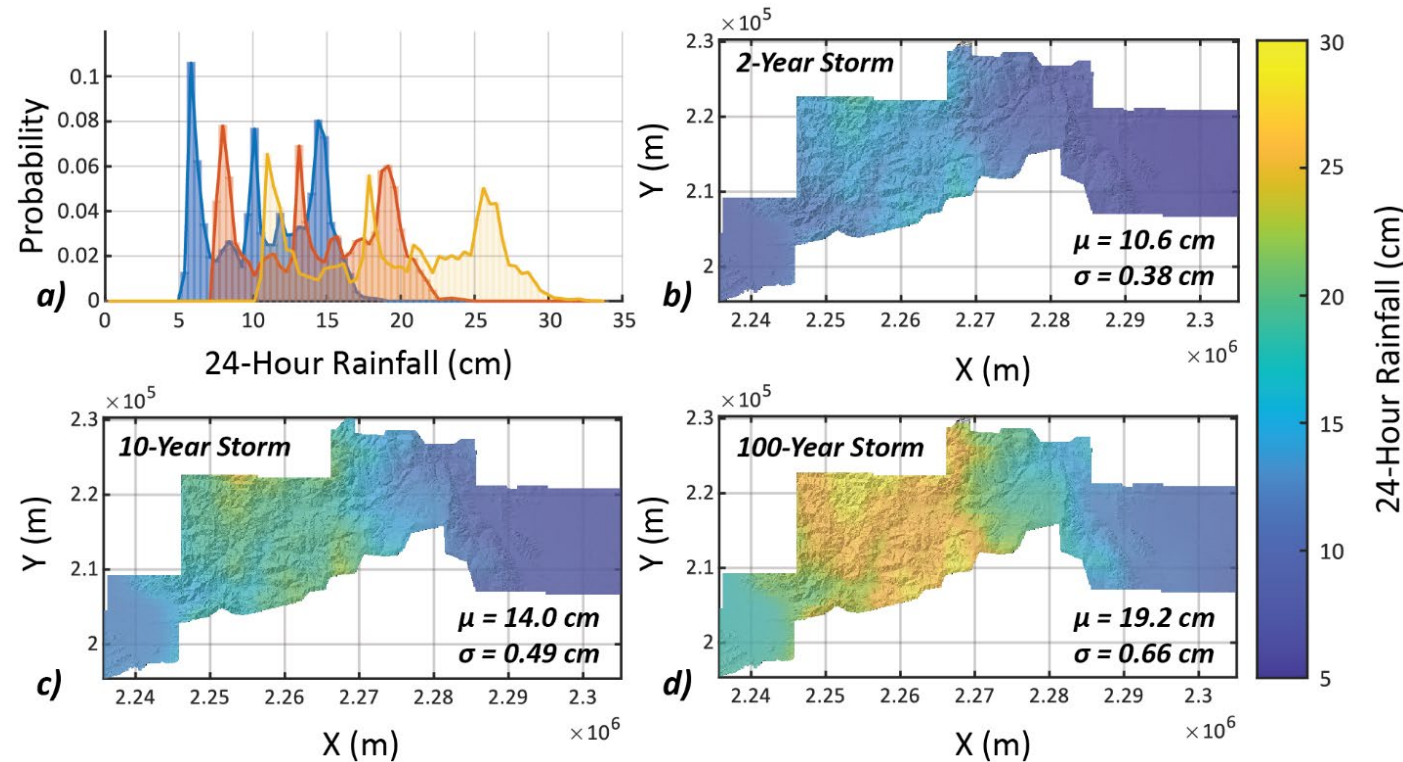
Inputs

- Strength
 - Distribution determined from forensics code.
- Soil Moisture, Unsaturated Properties
 - Soil moisture time series from NASA SMAP satellite data (daily)
 - SoilGrids, Rosetta GeoTransfer Function
- Estimated Soil Depth
 - Roering (2006) hillslope evolution model
- High-resolution DTM
 - OLC 3 ft. lidar, 1068 km²
- Intensity-duration precipitation for storm recurrence interval
 - ODOT hydraulics manual (e.g. 10 year storm)
- Seismic Event PGA map
 - OHELP, (Sharifi et al. 2016)



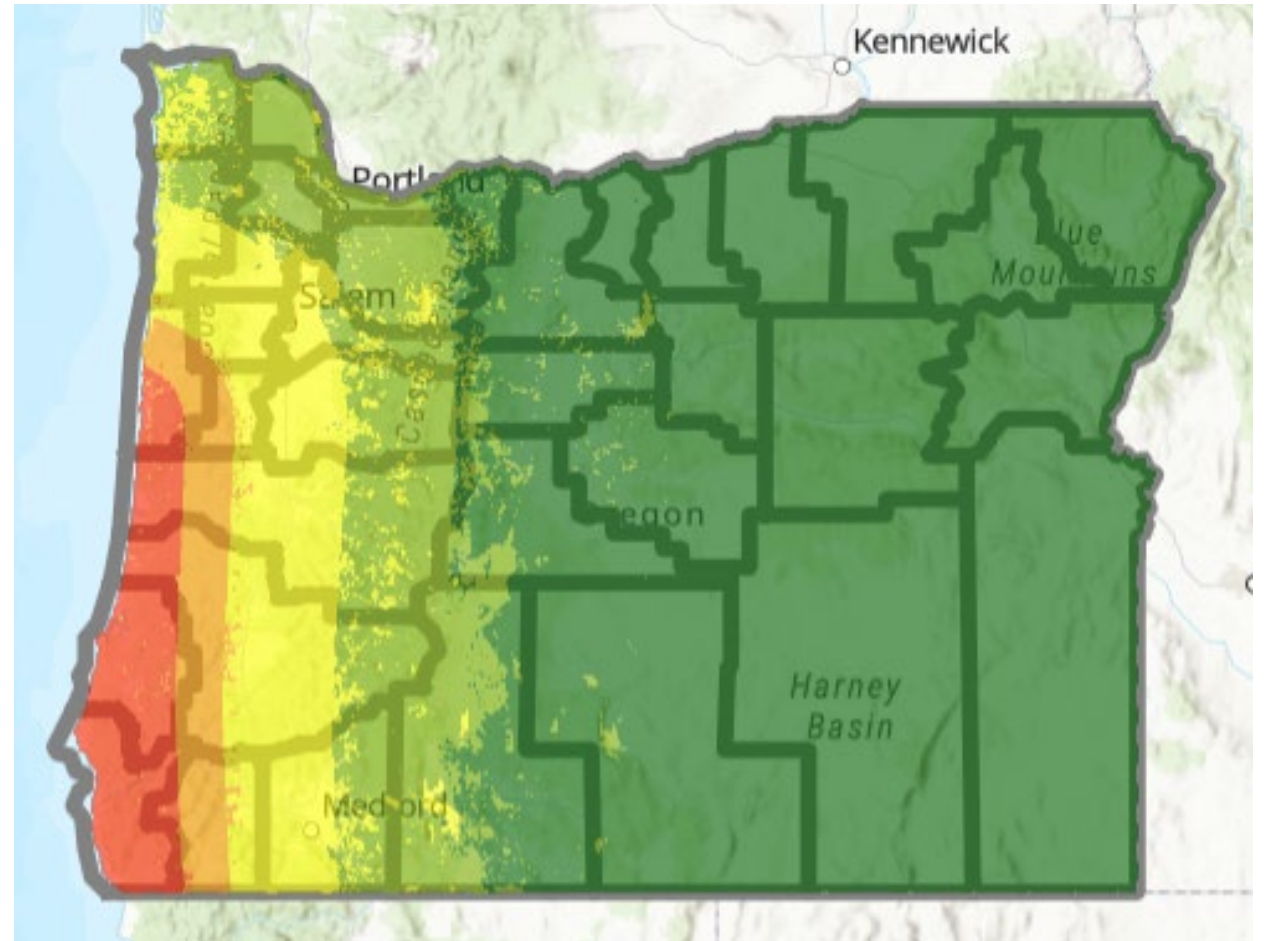
Inputs

- Strength
 - Distribution determined from forensics code.
- Soil Moisture, Unsaturated Properties
 - Soil moisture time series from NASA SMAP satellite data (daily)
 - SoilGrids, Rosetta GeoTransfer Function
- Estimated Soil Depth
 - Roering (2006) hillslope evolution model
- High-resolution DTM
 - OLC 3 ft. lidar, 1068 km²
- Intensity-duration precipitation for storm recurrence interval
 - ODOT hydraulics manual (e.g. 10 year storm)
- Seismic Event PGA map
 - OHELP, (Sharifi et al. 2016)



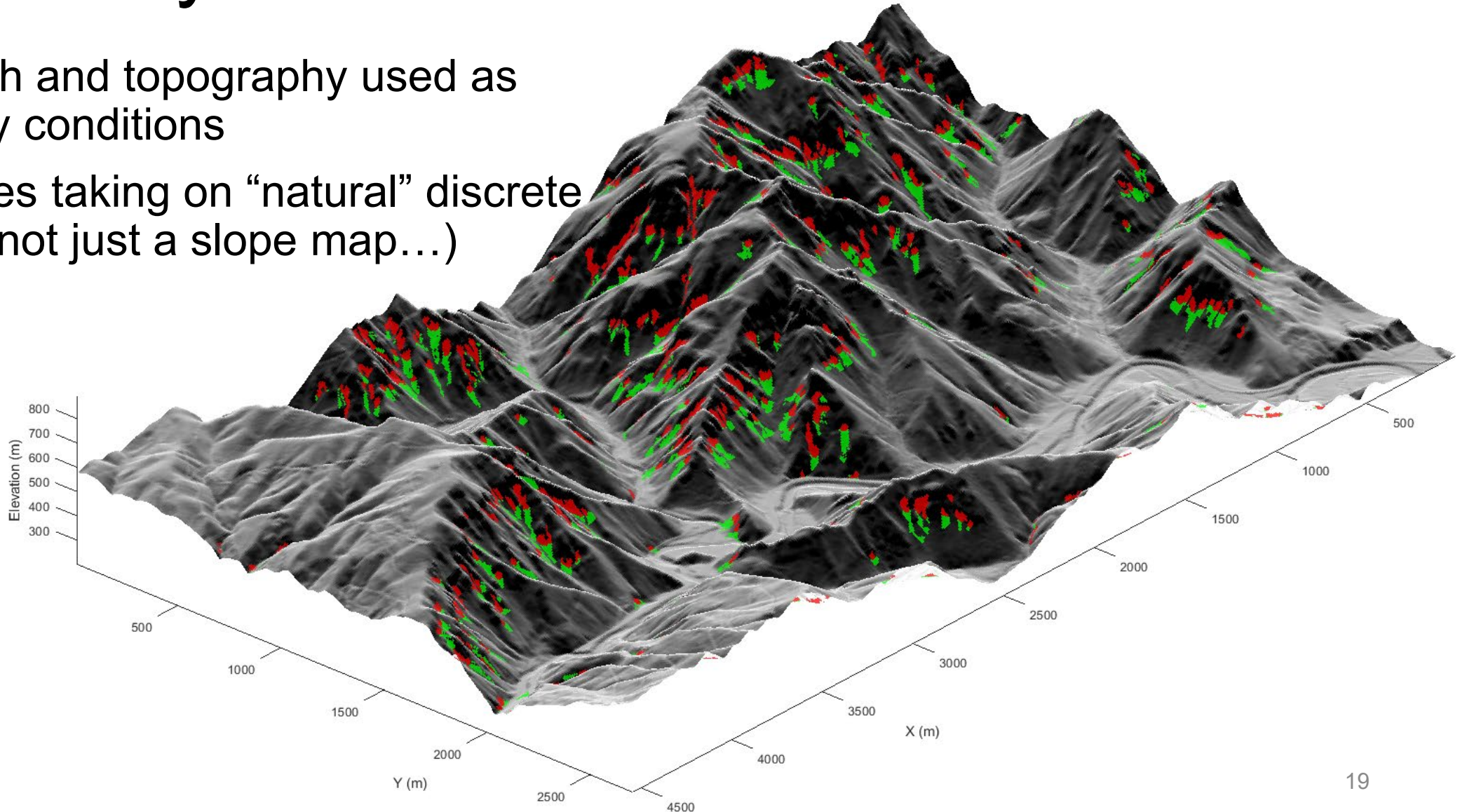
Inputs

- Strength
 - Distribution determined from forensics code.
- Soil Moisture, Unsaturated Properties
 - Soil moisture time series from NASA SMAP satellite data (daily)
 - SoilGrids, Rosetta GeoTransfer Function
- Estimated Soil Depth
 - Roering (2006) hillslope evolution model
- High-resolution DTM
 - OLC 3 ft. lidar, 1068 km²
- Intensity-duration precipitation for storm recurrence interval
 - ODOT hydraulics manual (e.g. 10 year storm)
- Seismic Event PGA map
 - OHELP, (Sharifi et al. 2016)



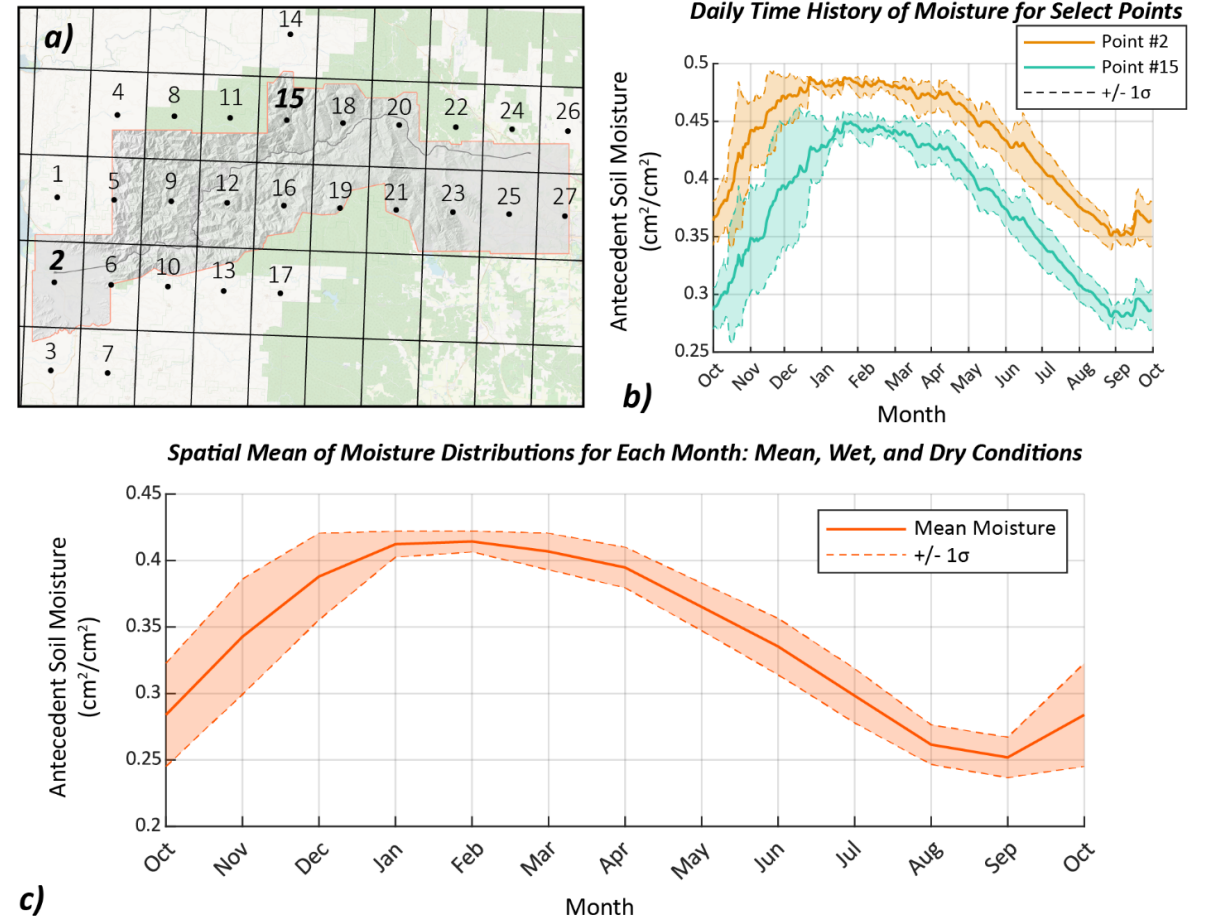
Susceptibility

- Soil depth and topography used as boundary conditions
- Landslides taking on “natural” discrete shapes (not just a slope map...)



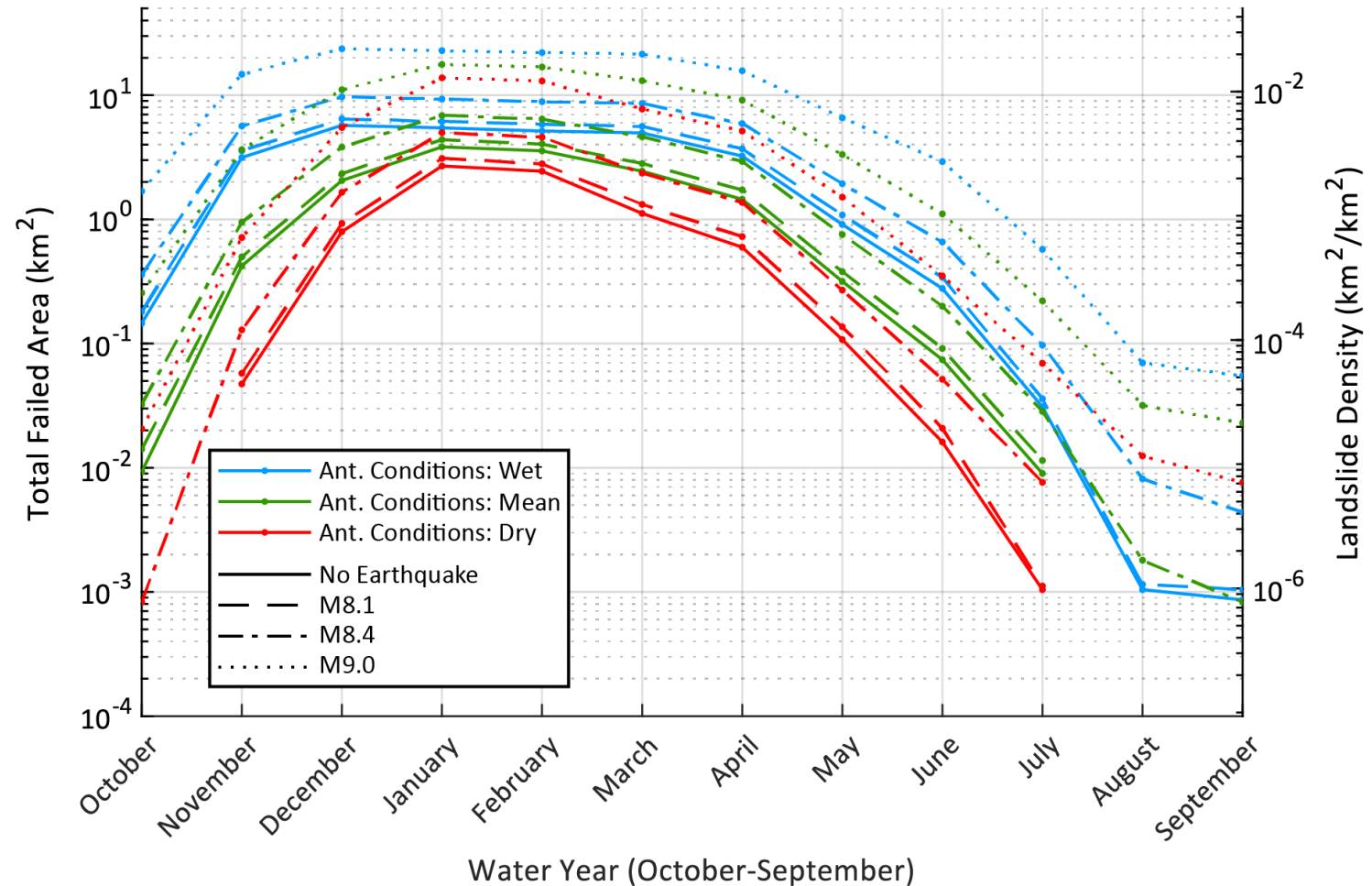
Role of Seasonality on Landsliding

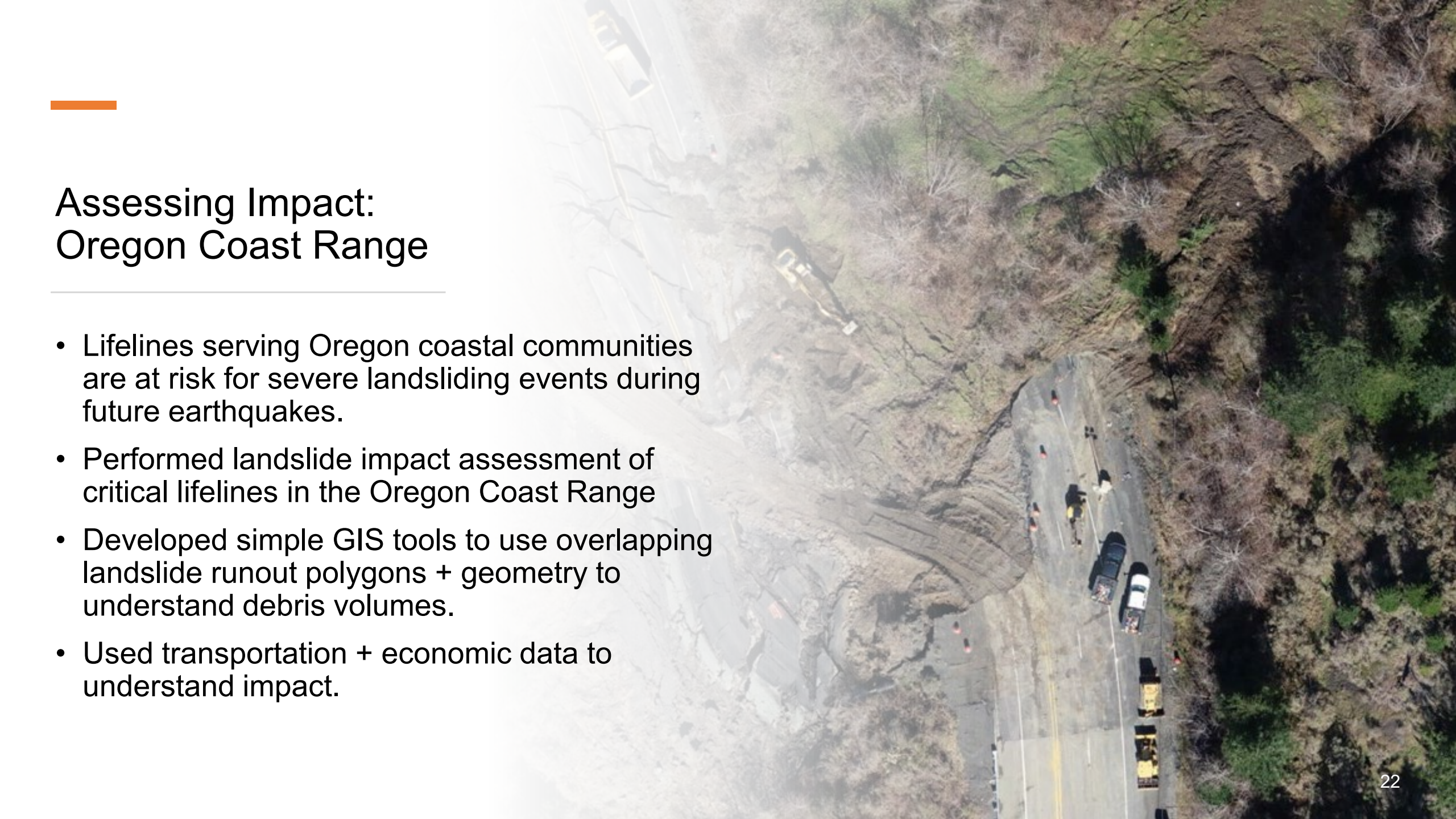
- Have you ever wondered...how would coseismic landslide impacts be different in the wet versus dry months?
- How much does the overall “wetness” of the winter matter in terms of landslide triggering events?
- These questions revolve around evaluating *antecedent* moisture conditions.



Does it matter when the “big one” happens?

- Landslide area density changes with seasonal antecedent soil moisture.
- Seasonality shows up to 2-4 orders of magnitude more landsliding in winter vs. summer months.
- Wet conditions vs. dry results in 2-12 times more coseismic landslides.
- The bigger the earthquake, more landsliding.



An aerial photograph showing a large landslide on a road. The landslide is a large, dark, irregular mass of earth and rock that has slid down a steep, vegetated hillside. The road is partially blocked by the landslide. Several vehicles, including a white van and a yellow truck, are stopped on the road. Orange traffic cones are placed around the landslide area. The background shows a road with a white van driving away from the landslide.

Assessing Impact: Oregon Coast Range

- Lifelines serving Oregon coastal communities are at risk for severe landsliding events during future earthquakes.
- Performed landslide impact assessment of critical lifelines in the Oregon Coast Range
- Developed simple GIS tools to use overlapping landslide runout polygons + geometry to understand debris volumes.
- Used transportation + economic data to understand impact.

Impact Assessment: Closure and Expense

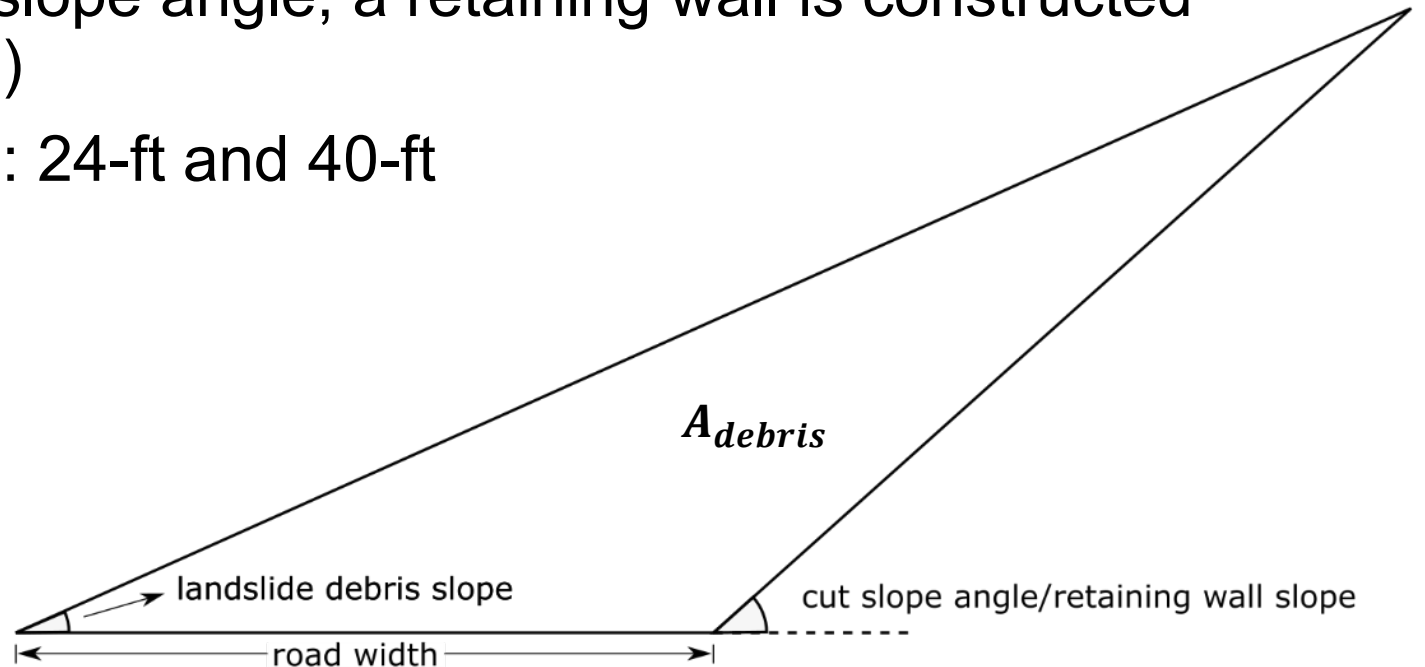
1. Use landslide clusters from susceptibility and associated runout to look at interaction with ODOT right-of-way (ROW)
2. Where landslides overlap ROW, time+cost of repair is assessed.
3. Result is time and cost of repair for each affected segment of highway and a total repair time and cost for entire corridor.



Repair Times and Costs – Debris Prism

- Create 3D prism of landslide debris on highway from lidar DEM
- Landslide debris slope = mean slope of superimposed landslide cluster
- Cut slope angle for emergency assumed to be 45°
- If landslide debris slope > cut slope angle, a retaining wall is constructed (small percentage of repairs...)
- Two highway widths assessed: 24-ft and 40-ft

$$V_{debris} = A_{debris}L_{hwy}$$



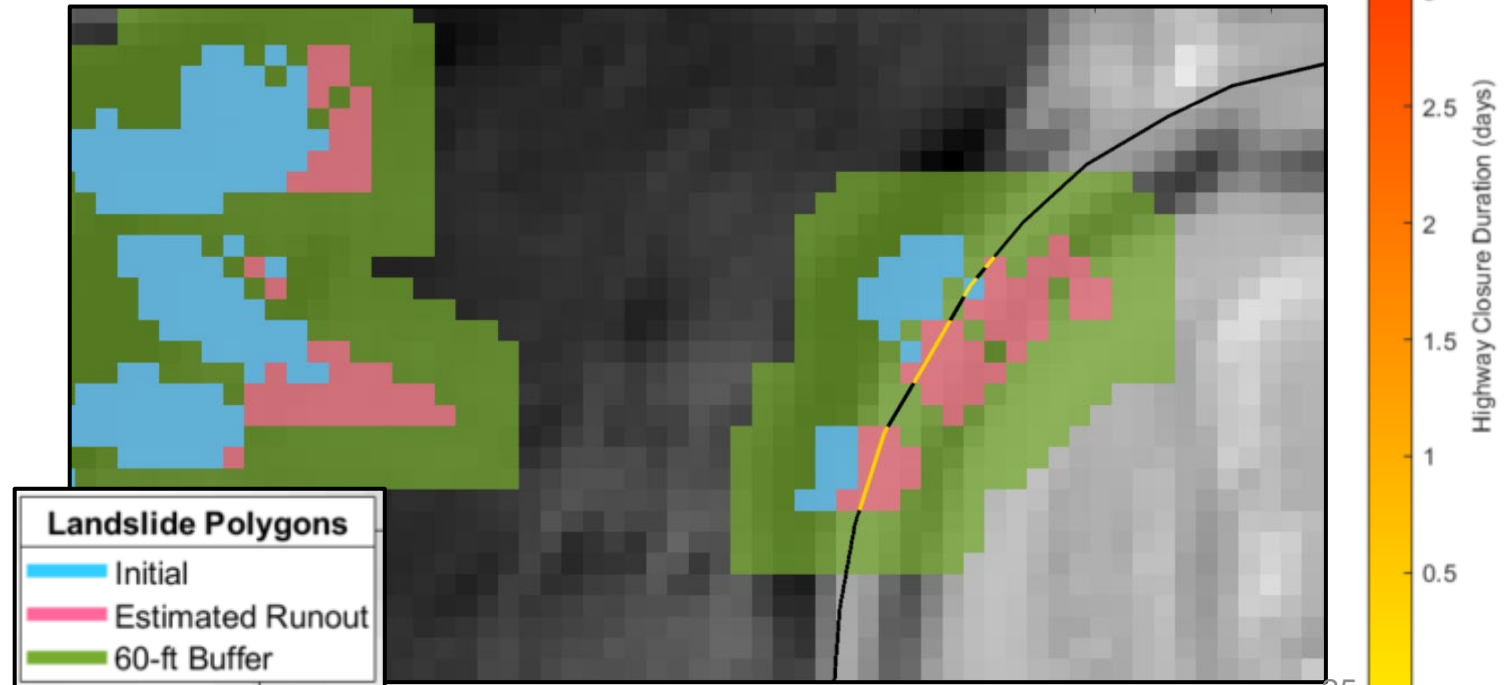
Repair Times and Costs – Duration of Closure

- Excavation rate:

$$R_{ex} = 5000 \text{ yd}^3 / \text{day} \text{ -or- } R_{ex} = 3600 \text{ m}^3 / \text{day}$$

- Duration of closure:

$$T_{closure} = \frac{V_{closure}}{R_{ex}}$$



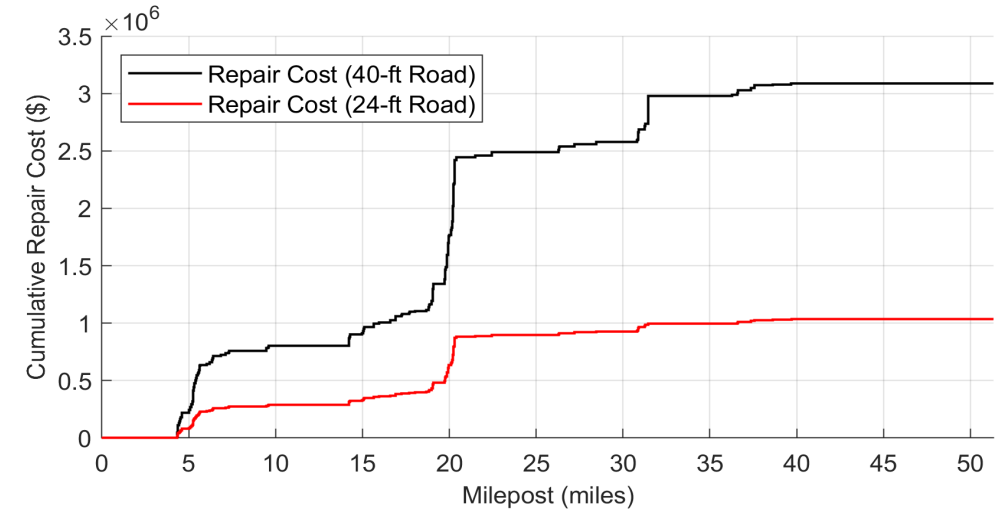
Repair Times and Costs – Cost of Closure

- Repair costs from:
 - ODOT Unstable Slopes Database (for standard cut slope repairs)
 - 2018 ODOT Bridge Cost Data Sheet for 2016-2018 (for retaining wall repairs)
- For cut slope/retaining wall repairs, cost of excavation: $C_{ex} = \$14.40/m^3$
- For retaining wall repairs, wall construction cost: $C_{wall} = \$59.20/ft^2$

$$C_{repair} = \begin{cases} V_{debris} C_{ex}, & \text{cut slope repair} \\ V_{debris} C_{ex} + A_{wall} C_{wall}, & \text{retaining wall repair} \end{cases}$$

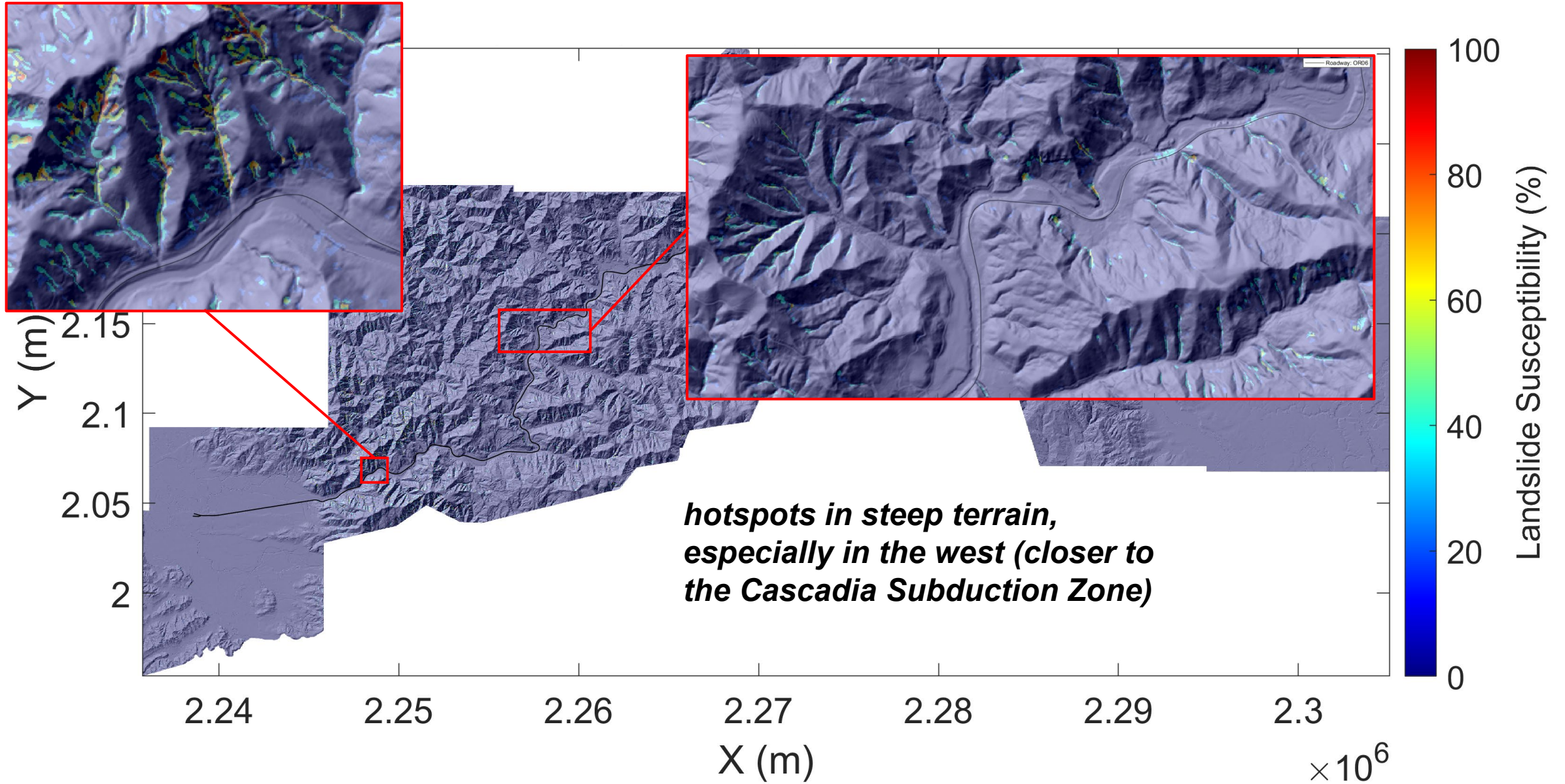
Repair Times and Costs – Cost of Closure

- Closure costs included in shapefile data for each corridor/scenario
 - May be easily mapped in GIS software by defining symbology by closure cost
- In report, costs are shown using profiles of milepost vs. cumulative repair cost:
 - Assuming both 24-ft and 40-ft width roadways
- Cost impacts generated using Transportation Planning and Analyses Unit (TPAU)

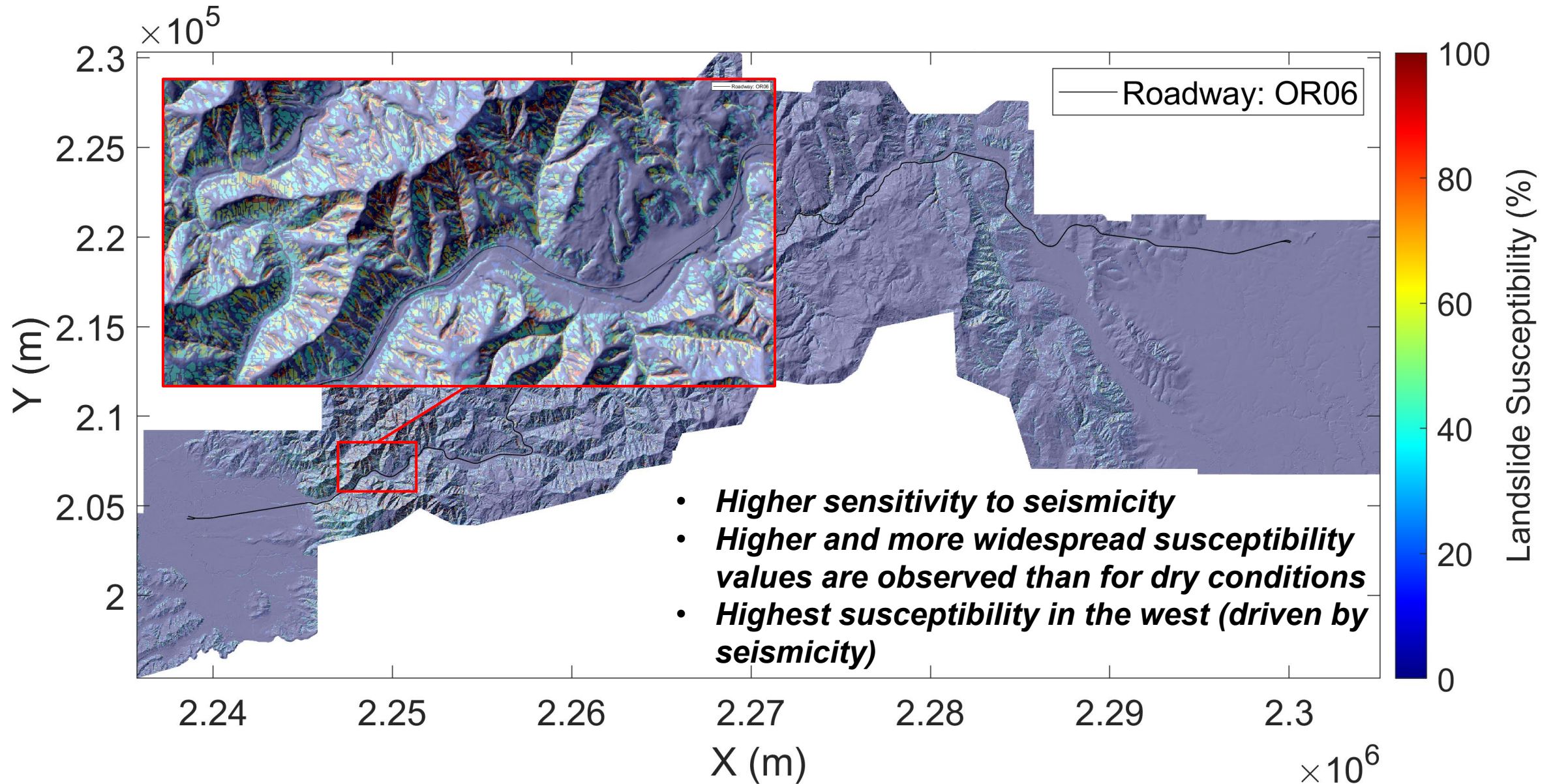


Daily Commodity Flow (USD)	
<i>OR06</i>	
Eastward	Westward
\$410,389	\$558,468
Average Daily Cost of Traffic Rerouting (USD)	
<i>OR06</i>	
\$109,658	

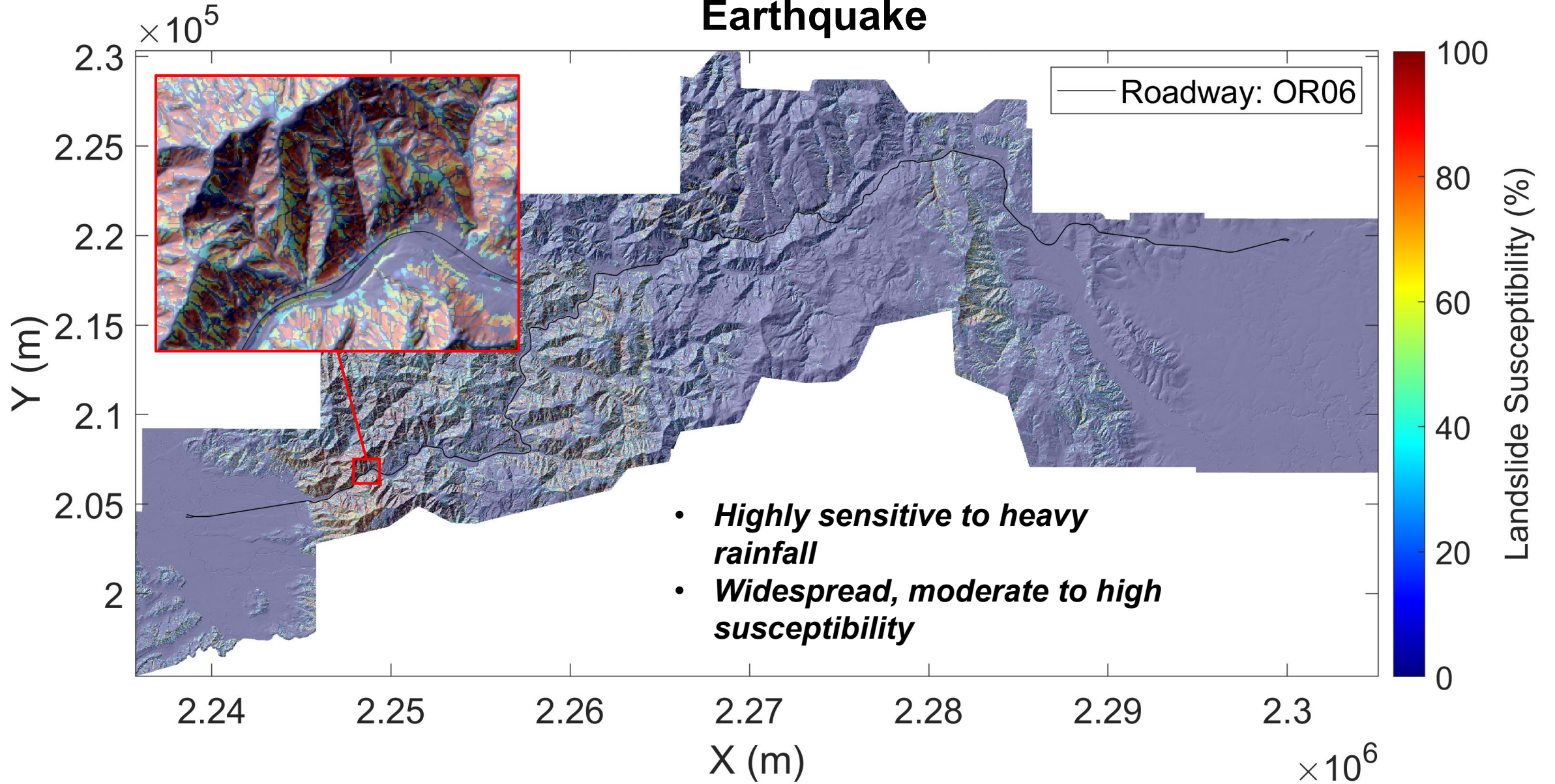
August Antecedent Conditions – M8.7 Earthquake



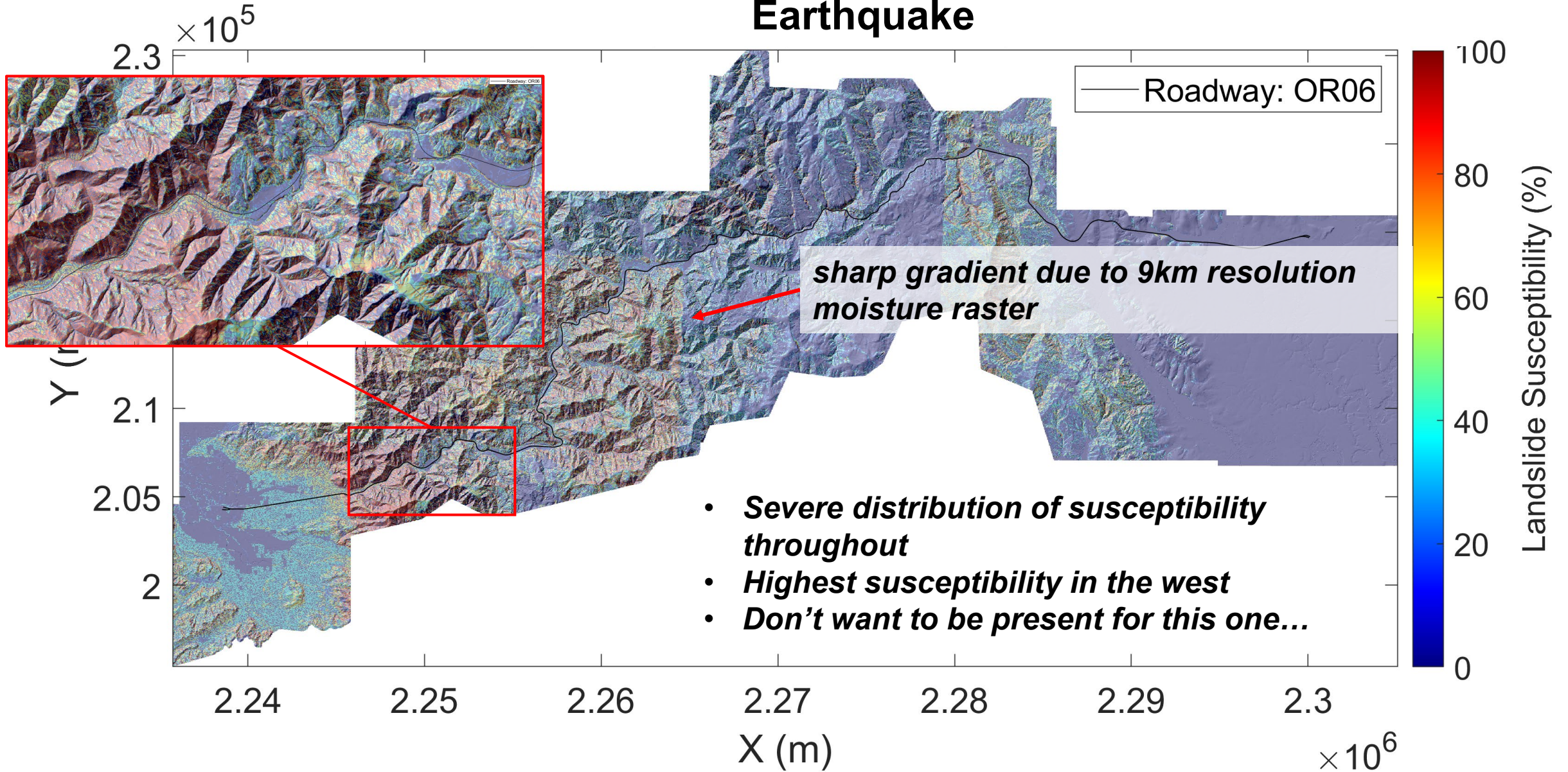
February Antecedent Conditions – M8.7 Earthquake



February Antecedent Conditions – 100-Year Storm - No Earthquake



February Antecedent Conditions – 100-Year Storm – M8.7 Earthquake



Susceptibility Observations

- Relatively stable in dry, summer conditions
- Susceptibility sensitive to moisture and rainfall, exacerbating susceptibility distribution during earthquakes
- Distribution of susceptibility varies depending on physical driver (e.g. rainstorm, seismicity, multi-hazard)

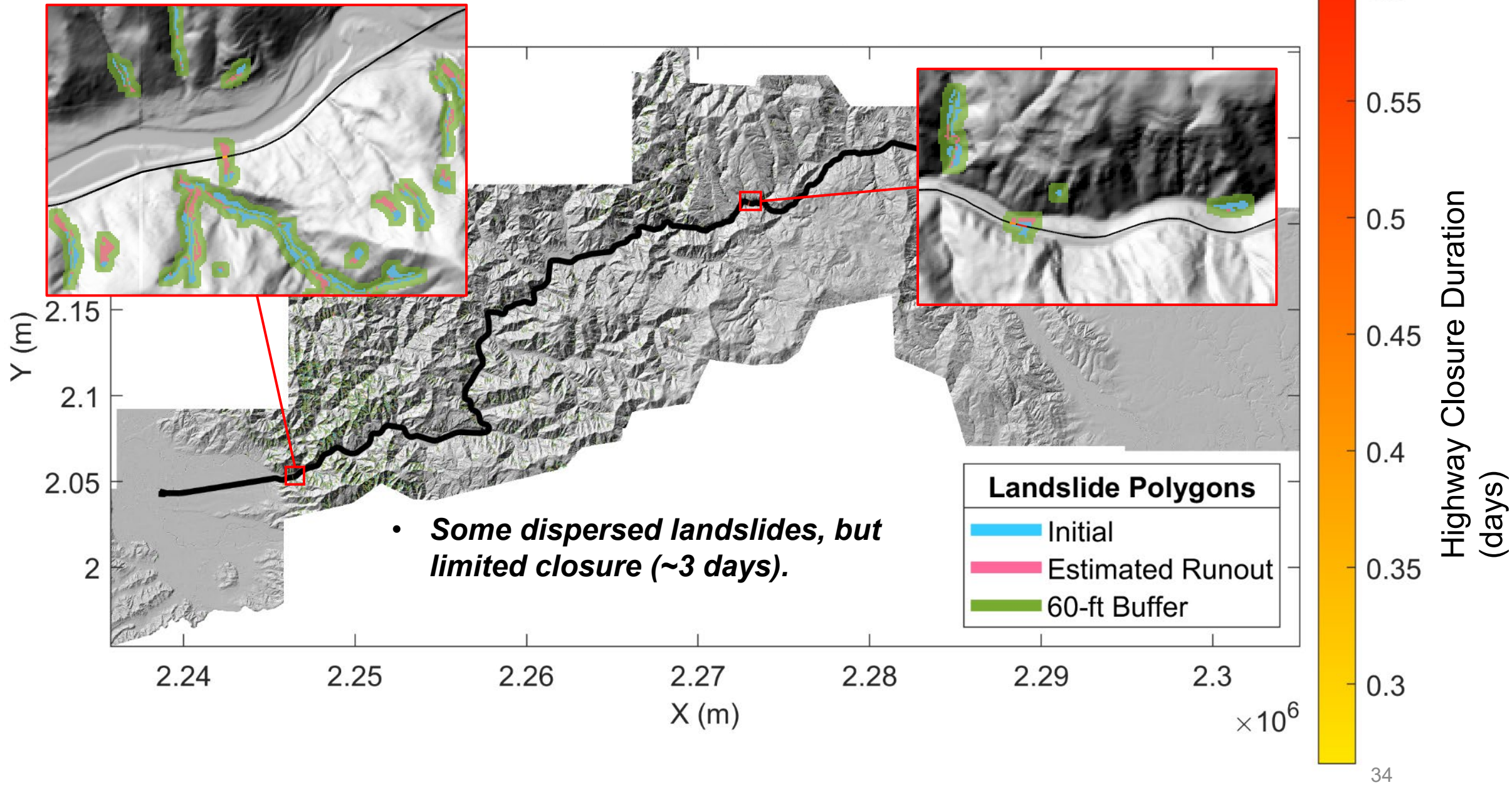


Risk Assessment

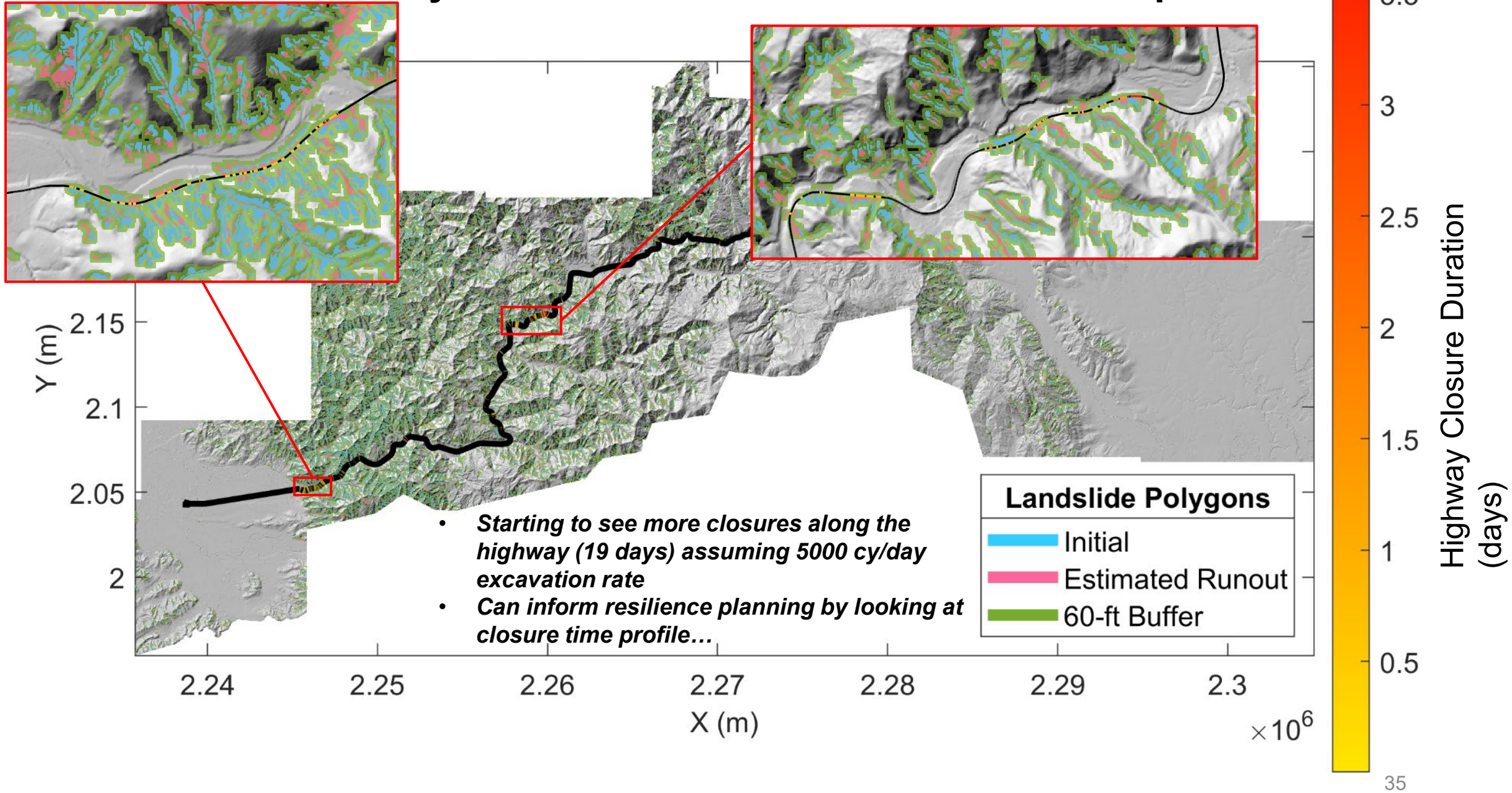
- Full suite of closure time maps, closure time profiles, and closure cost profiles available in SPR808 report
- Comprehensive table containing total closure times and costs, as well as event probabilities, commodity flow losses, and traffic rerouting costs available
- Shapefiles containing closure times and costs (all road widths and with/without 60-foot buffer)



August Antecedent Conditions – M8.7 Earthquake

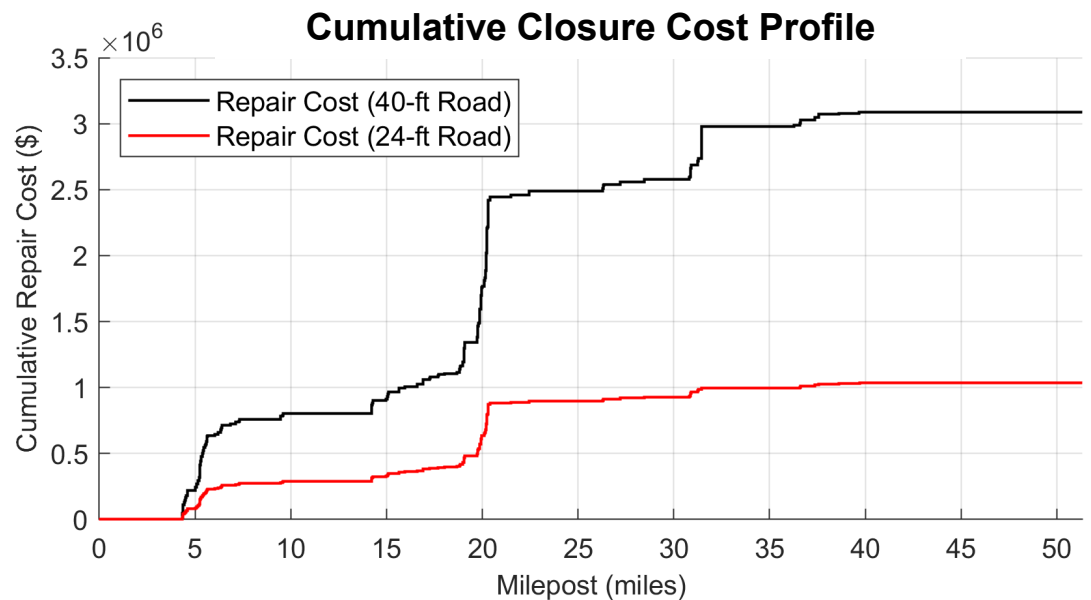
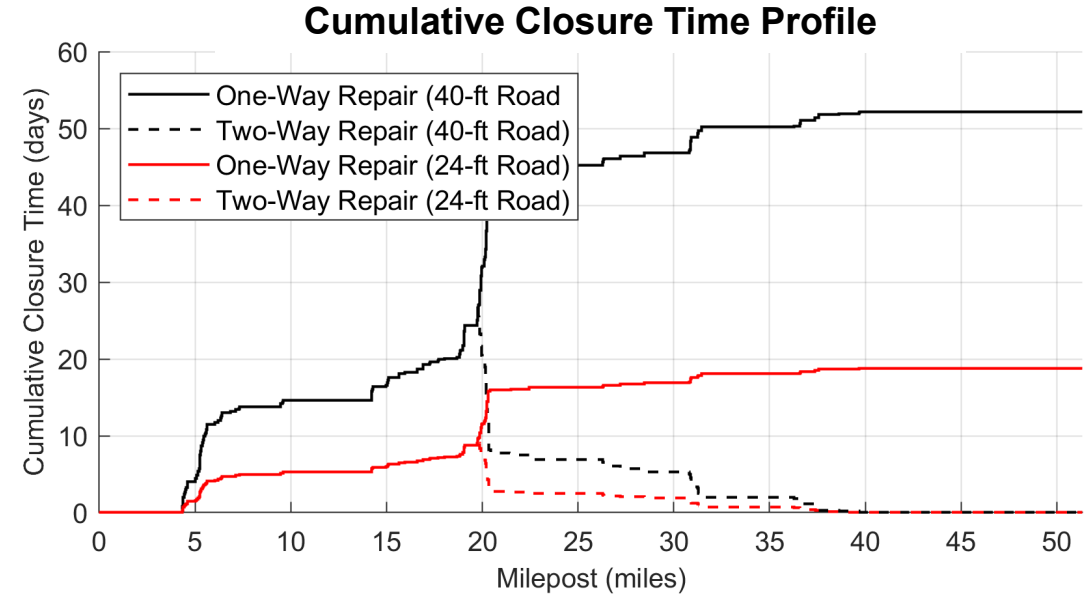


February Antecedent Conditions – M8.7 Earthquake

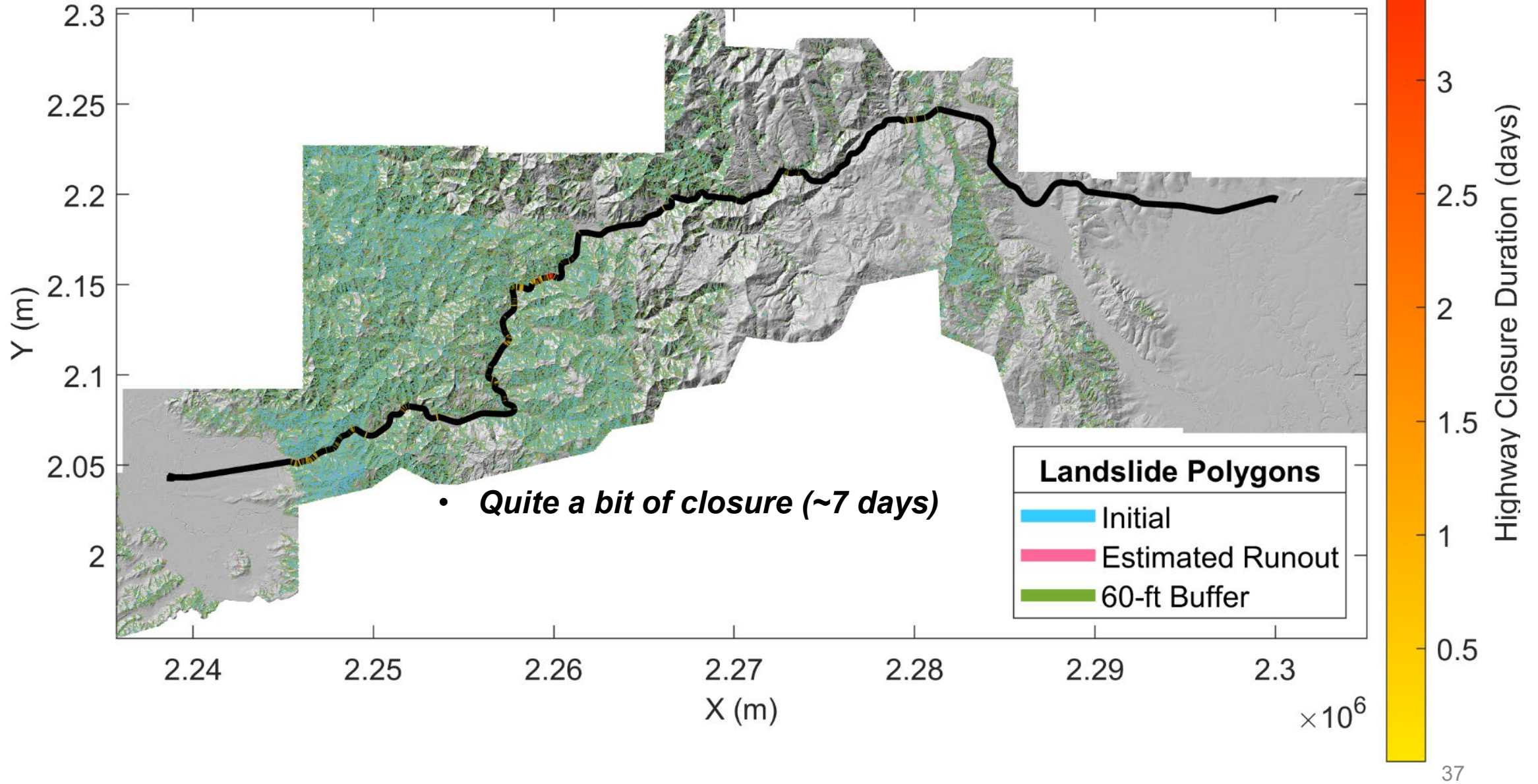


February Antecedent Conditions – M8.7 Earthquake

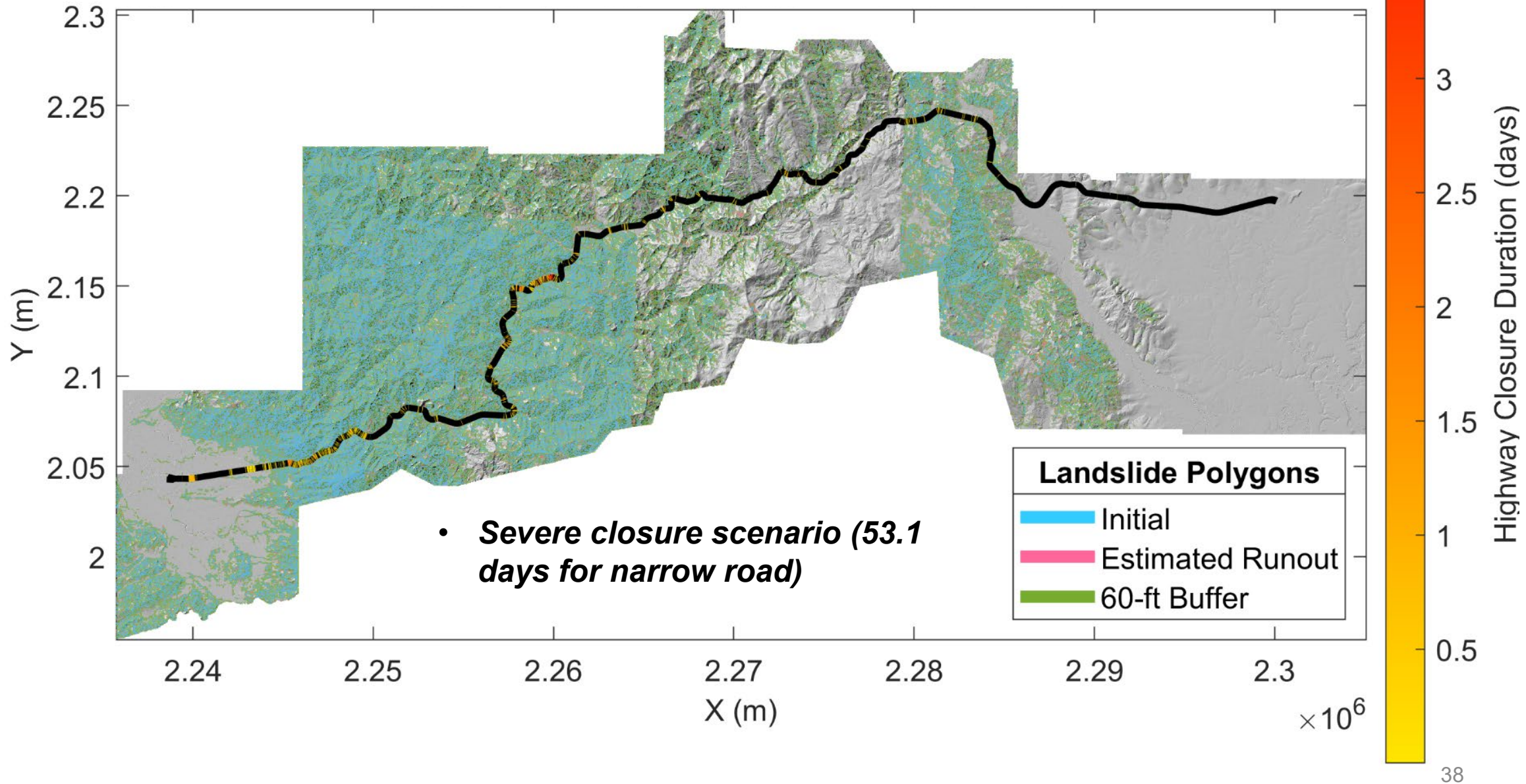
- Closed for:
 - 18.8 days (24-ft wide road)
 - 52.2 days (40-ft wide road)
- If repaired from both ends, time can ideally be reduced by half (dashed profiles)
- Cumulative cost shown as function of milepost



February Antecedent Conditions – 100-Year Storm - No Earthquake

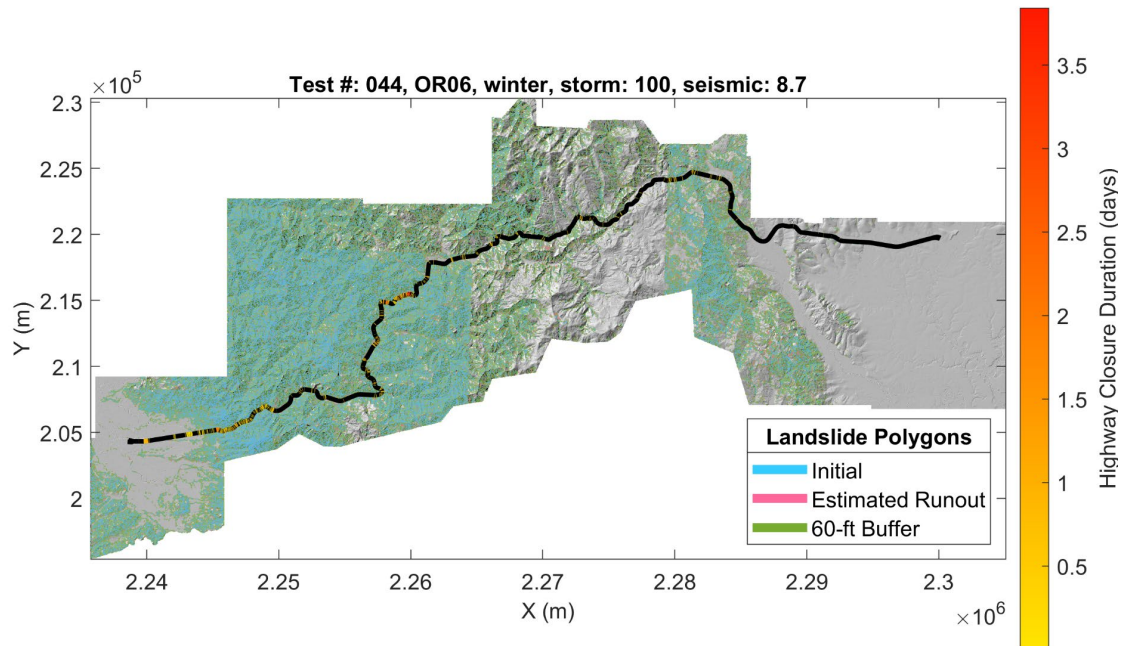


February Antecedent Conditions – 100-Year Storm – M8.7 Earthquake

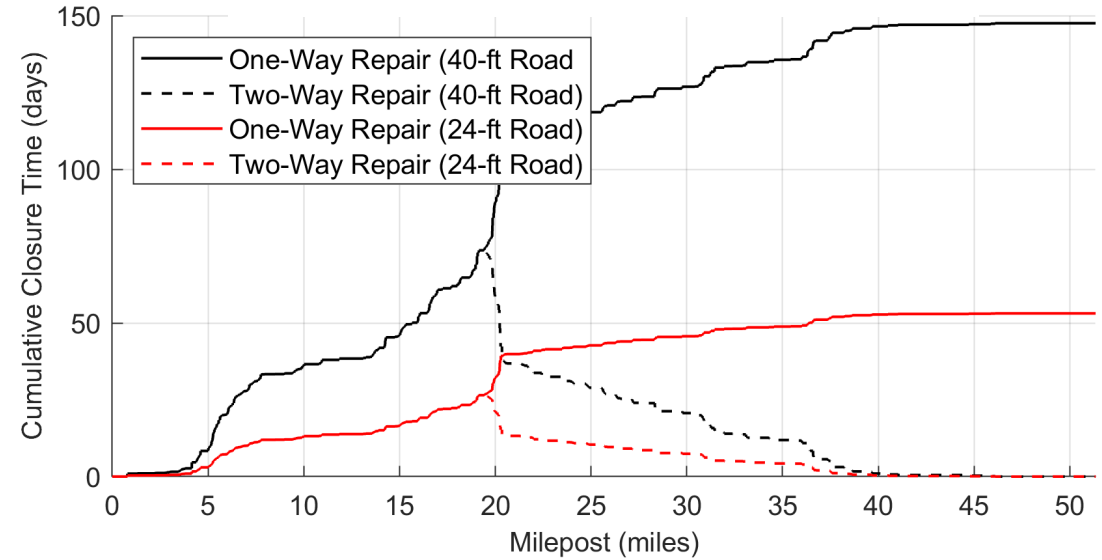


February Antecedent Conditions – 100-Year Storm – M8.7 Earthquake

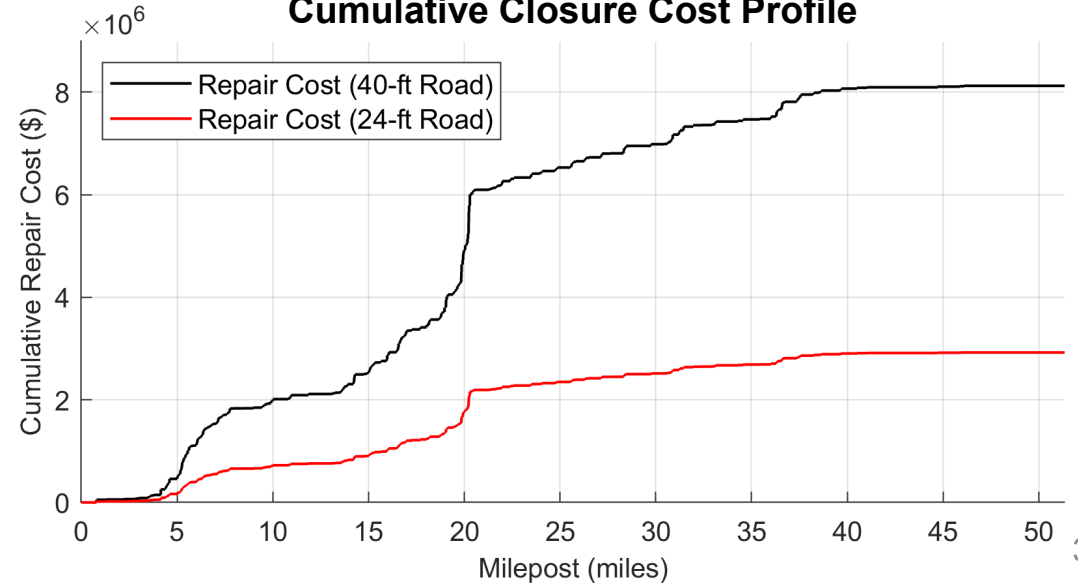
- Closed for:
 - 53.1 days (24-ft wide road)
 - 147.5 days (40-ft wide road)



Cumulative Closure Time Profile



Cumulative Closure Cost Profile



Scenario-Based ROW Impacts

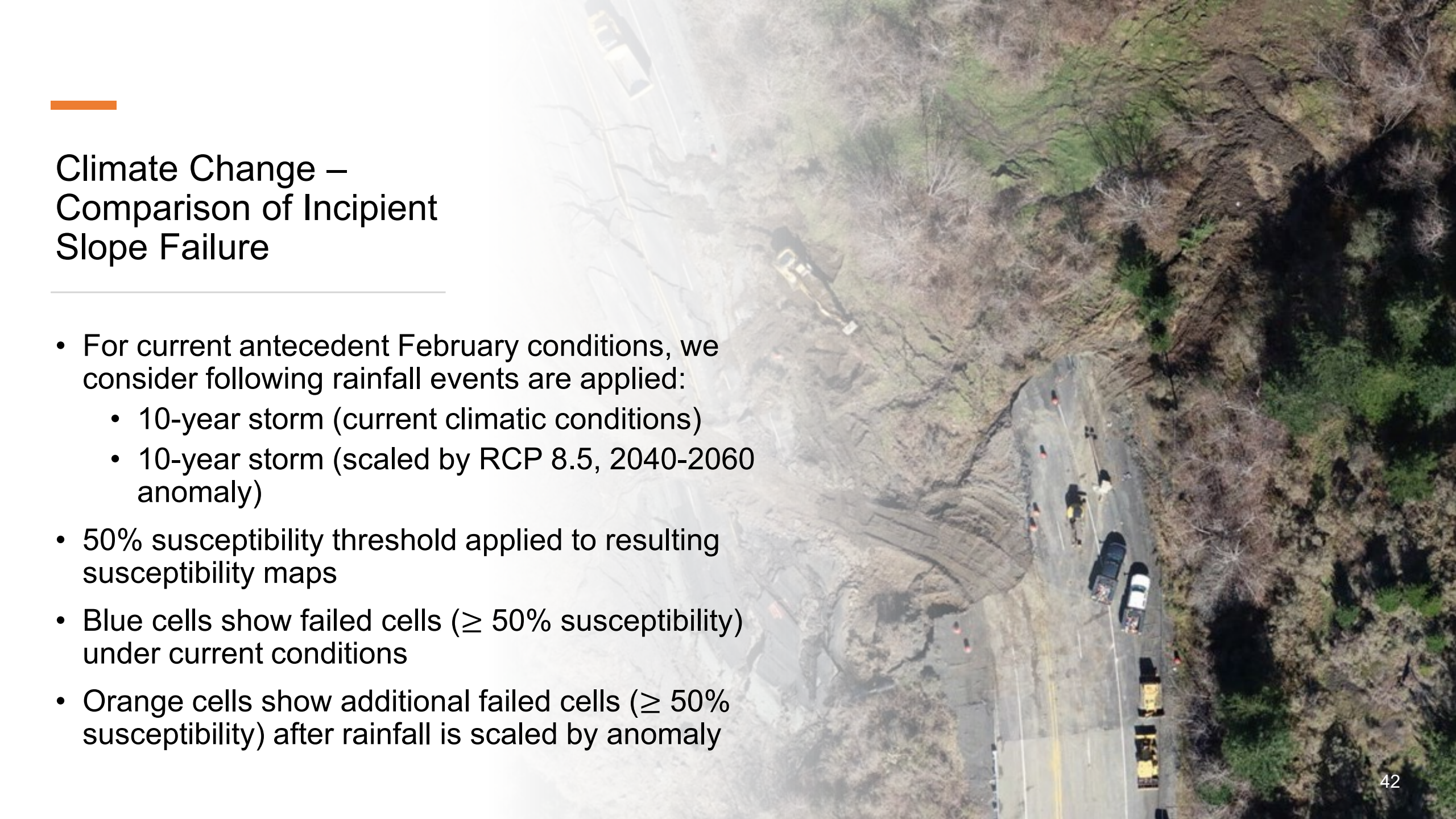
Test Information					Closure and Costs (40 ft Road Width)				Closure and Costs (24 ft Road Width)			
Test #	Highway	Season	Rainfall	EQ Moment Magnitude	Closure Duration (days)	Total Repair Cost (\$)	Commodity Loss (\$)	Rerouting Loss (\$)	Closure Duration (days)	Total Repair Cost (\$)	Commodity Loss (\$)	Rerouting Loss (\$)
1	US30	summer	off	off	7.47	\$411,091	\$17,105,522	\$1,669,133	2.69	\$211,745	\$6,157,988	\$600,888
4	US30	summer	off	8.7	33.03	\$1,818,072	\$75,650,136	\$7,381,835	11.89	\$722,501	\$27,234,046	\$2,657,460
6	US30	winter	off	off	125.22	\$6,968,623	\$286,832,704	\$27,988,736	45.08	\$2,763,962	\$103,259,768	\$10,075,943
9	US30	winter	off	8.7	131.93	\$7,528,488	\$302,182,880	\$29,486,582	47.49	\$3,017,910	\$108,785,832	\$10,615,168
16	US30	winter	100-year	off	122.65	\$7,261,696	\$280,935,552	\$27,413,298	44.15	\$2,855,909	\$101,136,792	\$9,868,785
19	US30	winter	100-year	8.7	172.72	\$9,947,466	\$395,614,336	\$38,603,492	62.18	\$3,946,541	\$142,421,152	\$13,897,256
26	OR06	summer	off	off	0.76	\$41,637	\$732,822	\$82,943	0.27	\$14,989	\$263,816	\$29,860
29	OR06	summer	off	8.7	1.65	\$90,703	\$1,596,401	\$180,686	0.59	\$32,653	\$574,704	\$65,047
31	OR06	winter	off	off	6.48	\$356,719	\$6,278,347	\$710,603	2.33	\$128,419	\$2,260,205	\$255,817
34	OR06	winter	off	8.7	52.17	\$3,089,513	\$50,546,760	\$5,721,043	18.78	\$1,312,383	\$18,196,832	\$2,059,576
41	OR06	winter	100-year	off	83.77	\$4,737,137	\$81,165,760	\$9,186,600	30.16	\$1,840,754	\$29,219,676	\$3,307,176
44	OR06	winter	100-year	8.7	147.53	\$8,121,059	\$142,932,512	\$16,177,555	53.11	\$2,923,581	\$51,455,704	\$5,823,921
51	US20	summer	off	off	0.00	\$0	\$0	\$0	0.00	\$0	\$0	\$0
54	US20	summer	off	8.7	0.00	\$0	\$0	\$0	0.00	\$0	\$0	\$0
56	US20	winter	off	off	6.47	\$355,918	\$8,953,142	\$1,208,077	2.33	\$128,130	\$3,223,131	\$434,908
						\$3,334,091	\$83,869,328	\$11,316,76	21.80	\$1,200,273	\$30,192,956	\$4,074,035

Climate Change Impacts on Shallow Landslides

- Climate change will result in wetter, warmer winters, more extreme rain events
- Current climatic conditions compared to future climate projection: RCP 8.5 (2040-2069)
- Impact on landsliding quantified as:
 1. Difference in number of failed cells
 2. Percent change in susceptibility for each DEM raster cell

Again, we will focus on corridor OR06, but a full suite of results are available in the report and in SPR808 report.

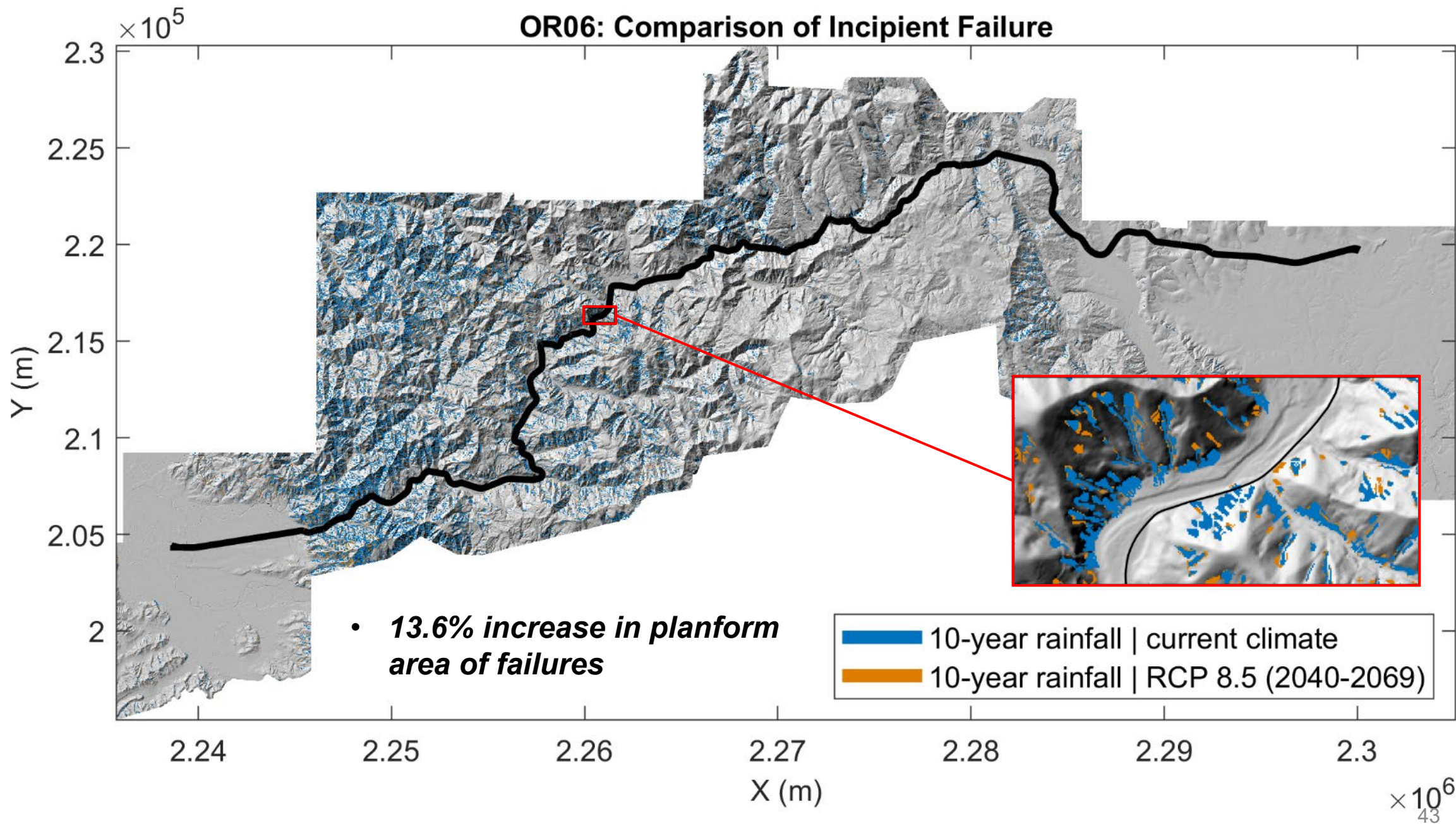


An aerial photograph showing a road on a hillside. A large area of the road and surrounding terrain has been covered by a landslide of earth and debris. Several vehicles, including a white van and a yellow truck, are stopped on the road. Orange traffic cones are placed around the affected area. The background shows a steep, vegetated hillside.

Climate Change – Comparison of Incipient Slope Failure

- For current antecedent February conditions, we consider following rainfall events are applied:
 - 10-year storm (current climatic conditions)
 - 10-year storm (scaled by RCP 8.5, 2040-2060 anomaly)
- 50% susceptibility threshold applied to resulting susceptibility maps
- Blue cells show failed cells ($\geq 50\%$ susceptibility) under current conditions
- Orange cells show additional failed cells ($\geq 50\%$ susceptibility) after rainfall is scaled by anomaly

OR06: Comparison of Incipient Failure



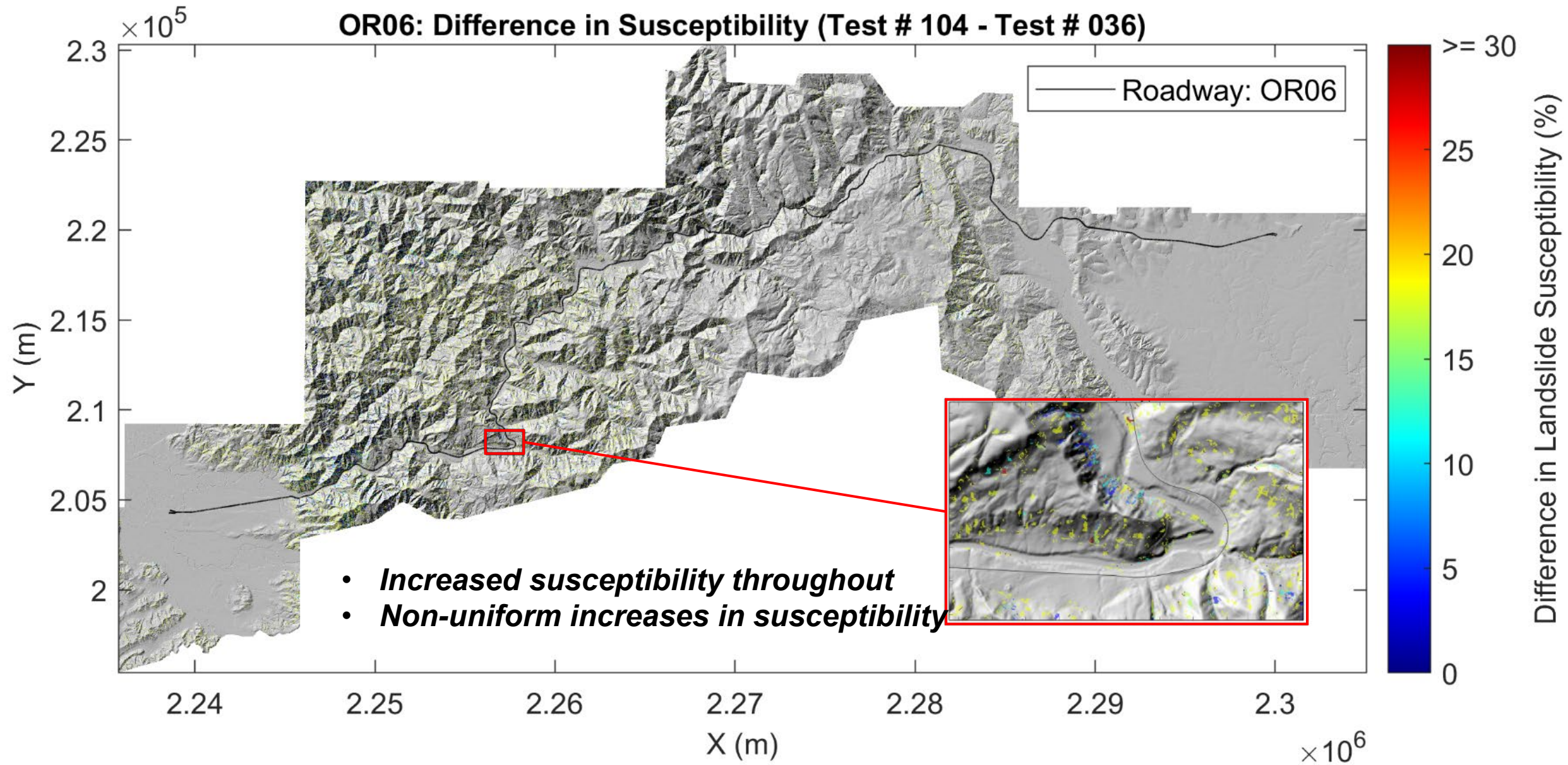
• **13.6% increase in planform area of failures**

- 10-year rainfall | current climate
- 10-year rainfall | RCP 8.5 (2040-2069)

Climate Change – Percent Change of Shallow Landslide Susceptibility

- For current antecedent February conditions, the following rainfall events are applied:
 - 10-year storm (current climatic conditions)
 - 10-year storm (scaled by RCP 8.5, 2040-2060 anomaly)
- Visual comparison of raw distributions of landslide susceptibility





Climate Change Assessment Summary

<i>Rainfall</i>	<i>Climatic Scenario</i>	<i>Failed Cell Area (km²)¹</i>	<i>% Increase in Failed Cell Area</i>	<i>Total Repair Cost^{2,3}</i>
US30				
	current	15.848		\$6,142,627
10-year	RCP 8.5 (2040-2069)	17.505	10.46%	\$6,187,891
	current	56.380		\$3,026,188
10-year	RCP 8.5 (2040-2069)	64.064	13.63%	\$3,234,754
US20				
	current	810.898		\$8,402,748
10-year	RCP 8.5 (2040-2069)	826.080	1.87%	\$8,485,809
OR42				
	current	6.260		\$581,940
10-year	RCP 8.5 (2040-2069)	6.839	9.25%	\$628,128

¹ Only incipient failure counted (landslide runout and buffer not included in count).

² Closure cost estimate includes estimated runout in analysis, but excludes landslide buffer.

³ Closure cost analysis assumes 40-foot (12.2-m) wide roadway.

Climate Change Assessment Conclusions

- Increased rainfall, due to climate change, will increase:
 - The area of landslides in the assessed corridors
 - The distribution of landslides in the assessed corridors
- The increase in susceptibility is non-uniform due to:
 - Spatial variability in:
 - Soil types
 - Rainfall magnitude
 - Rainfall anomaly
 - Variations in local topography
- Repair costs of ODOT right-of-way may see an increase in repair costs and closure times for 10 year storms that are closer to “current” 100 year storm conditions.
- Increase of 2-14% in landsliding rates.



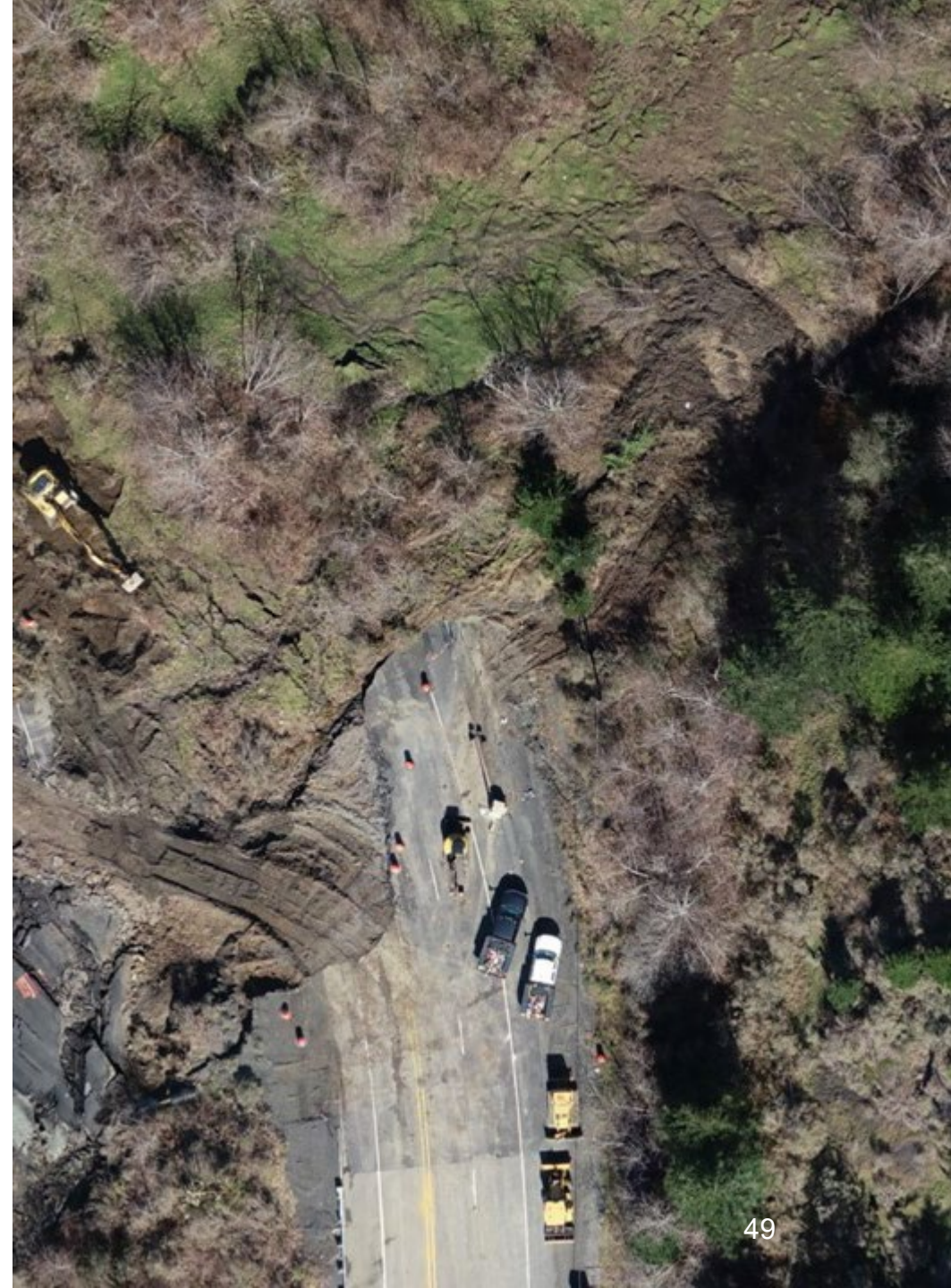
Conclusions: Applications of Susceptibility

- Susceptibility maps and TPAU outputs inform risk analyses, quantifying highway closure times and costs of highway repair, as well as commodity losses and costs tied to rerouting traffic during closure
- Corridors are shown to produce varying distributions of susceptibility depending on topography, antecedent moisture, rainfall events, seismic events, or multi-hazard events
- Susceptibility distributions driven by seismicity are shown to be exacerbated by high moisture and extreme storm events



Conclusions: Applications of Susceptibility

- Risk maps and risk profiles, showing the locations of closure “hot spots,” provide a glimpse of the potential impact of a large CSZ earthquake, suggesting that planners may:
 1. Place stockpiles of materials or equipment strategically to expedite post-disaster recovery
 2. Choose to implement mitigation techniques in areas that are unstable but of manageable size
 3. Make decisions regarding the scope of repairs in context of reopening and/or safety



Questions?

Acknowledgments

- Oregon Department of Transportation Projects:
 - ODOT-SPR-786
 - ODOT-SPR-807
 - ODOT-SPR-808
- People:
 - Curran Mohny, ODOT
 - Kira Glover-Cutter, ODOT
 - Nick Mathews, Mendenhall Fellow, USGS
 - Stefano Alberti, Post-Doc, Oregon State University
 - Michael Bunn, Cornforth Consultants, Inc.
 - Andrew Senogles, Ph.D., Oregon State University
 - Michael Olsen, Professor, Oregon State University
 - Oregon Lidar Consortium

